

DEVELOPMENT OF FULLY-PRINTED STRETCHABLE DEVICES

By

Yiheng Zhang

A THESIS

Submitted to
Michigan State University
in partial fulfillment of the requirements
for the degree of

Electrical Engineering – Master of Science

2018

ABSTRACT

DEVELOPMENT OF FULLY-PRINTED STRETCHABLE DEVICES

By

Yiheng Zhang

In recent years, stretchable flexible electronics has become a research hotspot in the electronics industry and academia due to its outstanding expansibility, adaptability, and portability. With the improvement of science and technology, materials science, mechanics, and manufacturing process have all achieved rapid development. Advanced technologies have made possible the manufacture of stretchable flexible electronic devices with excellent performance.

In the first half (chapter 2) of this thesis, we developed an inkjet printing method to pattern silver nanowires (AgNWs) with length of up to ~ 40 μm on various substrates. Well-defined and uniform AgNWs features could be obtained by optimizing the printing conditions including nozzle size, ink formulation, surface energy, substrate temperature, and printing speed. Such printed AgNWs have been used to demonstrate bi-axially stretchable conductors that could maintain stable conductance under an areal strain of up to 156% (256% of its original area). By printing the AgNWs electrodes on a composite composed of PDMS and electroluminescent (EL) phosphors, I have demonstrated a printed stretchable EL display. In chapter 3, I developed a silver nanoparticles (AgNPs) based stretchable sensor for pressure sensing through directly printing AgNPs on Polyurethane Acrylate (PUA) substrate. High sensitivity is indicated while I test it within a low-pressure load. Its resistance increases 100% when a 5.5 kPa pressure is applied on it. I explored the applications of heartbeat detection and wind sensing in this work.

ACKNOWLEDGMENTS

I would like to extend my most sincere gratitude to all who have given me care and help during my master's studies.

First of all, I feel very honored that Dr. Chuan Wang has accepted me into his team so that I get to work with incredible colleagues. His optimism, help, and encouragement has helped me discover the joy of scientific research. I would also like to thank my committee members: Dr. Wen Li and Dr. Nelson Sepúlveda for their valuable suggestions and kindly responding to my questions and doubts. Also I want to thank Dr. Tim Hogan for his advice on class selection when I just entered MSU and felt lost.

At the same time, I would like to thank the seniors of my group for their care and guidance. They are my guides on the academic road. When I first entered the laboratory, its Dr. Le Cai who passed on to me a lot of valuable experience and instrument operation methods. Thanks to Dr. Jinshui Miao, Dr. Suoming Zhang, Dr. Lei Zhang and Dr. Min Yu for their help and companionship. With them, I don't have to dine alone and conduct experiments alone. Thanks to Dr. Suoming for working out with me. Thanking Zhihao for letting me have tofu dumplings in the United States. I would like to thank Hongyang Shi as well. When I almost gave up after a dozen failures in making pressure sensors, he kept encouraging me and helping me. It is HongYang who made me understand that I must be patient with scientific research. Thanks Shuo Zhang for the help on the modification of format on this dissertation.

In the end, I want to thank my parents for giving me unconditional trust and support. Without their love I wouldnt have made it here.

TABLE OF CONTENTS

LIST OF TABLES	v
LIST OF FIGURES	vi
CHAPTER 1 INTRODUCTION	1
1.1 Background	1
1.1.1 Flexible and Stretchable Electronic Devices	1
1.1.2 Printing Method Applied in Device Fabrication	10
1.1.2.1 Printing Technology	10
1.1.2.2 Printing Materials	13
1.1.2.3 Inkjet Printing	15
1.2 Contributions	16
1.3 Thesis Organization	17
CHAPTER 2 DIRECT PRINTING FOR ADDITIVE PATTERNING OF SILVER NANOWIRES FOR DISPLAY APPLICATION	19
2.1 Introduction	19
2.2 Design and Fabrication Method	21
2.3 Test	22
2.3.1 Measurement Setup	22
2.3.2 Experimental Results and Analysis	22
2.4 Application	28
2.5 Conclusion	31
CHAPTER 3 INKJET-PRINTED STRAIN SENSOR FOR PRESSURE SENSING .	32
3.1 Introduction	32
3.2 Design and Fabrication Method	34
3.3 Experimental Results and Analysis	35
3.4 Application	41
3.4.1 Heart Rate Detection	42
3.4.2 Wind Sensing	44
3.5 Conclusion	45
CHAPTER 4 SUMMARY AND FUTURE WORK	46
4.1 Summary	46
4.2 Future work	46
BIBLIOGRAPHY	48

LIST OF TABLES

Table 1.1: Comparison of various fabrication technology	11
---	----

LIST OF FIGURES

Figure 1.1:	schematic of the cross-section of an organic transistor circuit technology based on flexible printed wiring boards.[12]	2
Figure 1.2:	(a) Schematic of the island-bridge structure with serpentine geometry; (b) optical image of the as fabricated serpentine structures.[16]	4
Figure 1.3:	The dynamically tunable electronic eye camera from the team of John A. Rogers. [39]	6
Figure 1.4:	Paper smart phone and flexible display that HP exhibited in MobileBeat conference.[48] [49]	7
Figure 1.5:	Tattoo-based platform for noninvasive glucose sensing. (A)Schematic of the printable iontophoretic-sensing system displaying the tattoo-based paper (purple), Ag/AgCl electrodes (silver), Prussian Blue electrodes (black), transparent insulating layer (green), and hydrogel layer (blue). (B) Photograph of a glucose iontophoretic-sensing tattoo device applied to a human subject. (C) Schematic of the time frame of a typical on-body study and the different processes involved in each phase.[50]	8
Figure 1.6:	Electrical performance of nanomesh conductors on skin and their sensor applications. a, b, Conductance of nanomesh conductors attached to a finger when the hand is opened and closed. c, Depiction of an on-skin wireless sensor system. Electrical signals are transmitted from the fingertip to a wireless module through on-skin nanomesh conductors, anisotropic films and conductive threads. The electrode array acts as a touch sensor for conductive materials. It can also be used as a thermal and/or pressure sensor when polymer PTC and pressure-sensitive rubbers are attached, respectively. d, f, Electrical performance of touch (d), temperature (e) and pressure (f) sensors. The inset shown in (e) shows the thermal sensor laminated onto a silicone replica substrate with nanomesh conductors. Scale bars, 3 mm.[51]	9
Figure 2.1:	schematic diagram illustrating the printing process.[118]	23
Figure 2.2:	(a) MSU shaped AgNW patterns printed on PDMS. Scale bar: 1 cm. (b) Straight line patterns of AgNWs printed on silicon wafer, glass slide, polyimide thin film and VHB tape. Scale bars: 2 cm.[118]	24
Figure 2.3:	Optical micrograph (top) and SEM image (bottom) of the AgNW network printed on Si wafer. Scale bars: 50 μ m and 1 μ m, respectively.[118]	25

Figure 2.4:	Electrical and electromechanical characterization of the printed AgNW features with different nanowire lengths. (a) SEM images of the AgNW network with average nanowire length of ~ 4.4 m, ~ 15.6 m and ~ 38.5 m (from top to bottom). Scale bar: 5 m. (b) Nanowire length distribution of the three different AgNW inks. (c) Feature resistance as functions of number of printing runs for AgNWs with different nanowire lengths. Inset, same data presented in log scale. (d) Resistance as a function of printed feature length for all three kinds of AgNW inks. (e) Relative change in resistance as a function of tensile strain for features with average nanowire lengths of ~ 38.5 m and ~ 4.4 m. (f) Cyclic stretching test results for the feature with an average nanowire length of ~ 38.5 m. Inset, measurement setup. Scale bar: 1 cm.[118]	26
Figure 2.5:	Bi-axially stretchable conductors based on the printed AgNWs. (a) Feature resistance as functions of areal tensile strain (top) and stretching cycles (bottom) for a AgNW feature printed on a bi-axially pre-stretched PDMS substrate. Insets: the sample at relaxed state (left) and being stretched to an areal strain of 125% (right). (b) The current-voltage (I-V) curves of the LED-driving circuit using the printed bi-axially stretchable AgNW conductor as interconnect with the areal strain varying from 0% to 156%. Insets: photographs of the circuit while the interconnect is under 0 (left) and 125% (right) areal tensile strain. Scale bar: 2 cm.[118]	27
Figure 2.6:	Stretchable electroluminescent (EL) displays using the printed AgNWs as electrodes. (a) Schematic of the device structure. (b) EL spectra of the device made of green phosphors under different stimulation conditions. (c, d) EL intensity of the device made of green phosphors as functions of frequency (c, measured at 1 kV) and magnitude (d, measured at 500 Hz) of the AC voltage. (e) Normalized EL intensity plotted as a function of tensile strain when measured under AC voltage with different magnitudes and a frequency of 1 kHz. Inset: photographs of a device made of green phosphors under 0 and 20% tensile strains. Scale bars: 5 mm. (f) Normalized EL intensity versus stretching cycles measured under AC voltage with a magnitude of 1.5 kV and a frequency of 1 kHz. (g) Photographs of a 66 EL display array made of green phosphors (left), an MSU display pattern using orange, green and blue phosphors for M, S and U, respectively (middle), and the MSU-shaped display under 0 and 20% tensile strains (right). Scale bars: 1 cm.[118]	30
Figure 3.1:	Capacitive soft pressure sensor array based on PEDOT:PSS (scale bar, 20 mm). (a) Device structure. (b) Capacitance change in response to pressure.[151]	34
Figure 3.2:	Schematic diagram of printing process and device pattern.	35

Figure 3.3: A sample of printed pressure sensor.	36
Figure 3.4: Pressure loading platform for measurement.	37
Figure 3.5: Force-to-voltage response curve of the FSR.[151]	37
Figure 3.6: Pressure sensor based on printed AgNPs. (a) Relative change in resistance and pressure as a function of time. (b) Relative change in resistance as a function of pressure.	39
Figure 3.7: (a) Optical image of the device before test (b) Optical image of the device after test.	40
Figure 3.8: The relative change in AgNPs patterns resistance under different pressure loading frequency.	41
Figure 3.9: Heart rate sensing test.	42
Figure 3.10: Heart rate sensing: resistance of sensor as a function of time.	43
Figure 3.11: Windspeed sensing test. (a) Measurement setup. (b) Fixture for sample in wind tunnel. (c) Relative change in sensor resistance as a function of windspeed.	44

CHAPTER 1

INTRODUCTION

Flexible electronics [1] represents a new kind of electronic technology that has been widely used in many fields. Evolving thin-film materials and devices have brought great progress in various applications to flexible electronics. The large-area, low-cost manufacturing process has endowed flexible electronics with unique flexibility and extensibility. It shows us broad application prospects in almost all fields including information, energy, medical, and national defense. Moreover, many devices have been developed such as flexible transistors, which have already been commercialized [2, 3, 4] large area printed pressure sensors [5], RFID tags [6], which have been put into wide application, soft solar cell [7], and a light emitting diode (LED) application, etc. The flexible electronics applications have been covered from the biomedical field energy to space science and art [8, 9].

1.1 Background

1.1.1 Flexible and Stretchable Electronic Devices

Current general-purpose conventional electronic devices are generally fabricated on a rigid substrate like a silicon wafer, and their hard and brittle nature makes it difficult for the electronic devices to bend or extend. Once there is a large deformation applied, the structure of the electronic devices will be destroyed or the performance will be compromised. Therefore, it is difficult for conventional electronic devices to adapt to the high requirements of the next generation electronic products in terms of convenience and flexibility, and it is urgent to find a method that can realize the flexibility of electronic devices. In 1998, the ordered buckling of metal thin films on an elastic substrate was first proposed by N. Bowden et al.[10]. The study of the flexibility of electronic devices began with the study of organic electronics [11]. People hoped to use organic semiconductors to replace traditional silicon materials. Scien-

tists at Bell Labs [12] combined thin-film transistors with flexible substrates to implement electronic circuits at a clock frequency of 1 kHz. Figure 1.1 shows the schematic of the cross-section of an organic transistor circuit technology based on flexible printed wiring boards used in that study.

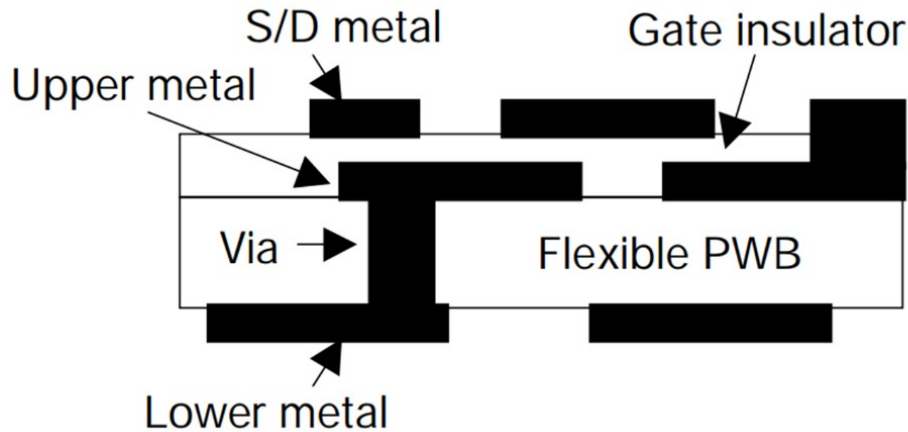


Figure 1.1 schematic of the cross-section of an organic transistor circuit technology based on flexible printed wiring boards.[12]

In 2004, Professor S. R. Forrest [13] of Princeton University reviewed the research status and development direction of organic electronics, proposed a conceptual design and manufacturing method, and demonstrated a pen-shaped flexible display. However, organic semiconductors have quite different physical and electrical properties compared with silicon-based semiconductors. This severely restricts the practical and industrialization of organic electronics and makes it difficult for the study of organic electronics to move forward.

In recent years, with the continuous development of mechanics, materials science, and manufacturing process levels and by improving the traditional manufacturing processes and methods of silicon electronic devices, it is now feasible to manufacture stretchable flexible electronic devices, which has good portability and adaptability, as well as the ability to maintain good performance under tension, compression, bending and twisting. Instead of replacing the current silicon chip technology, current flexible electronic technology is not an improvement on the silicon substrate structure. Mostly it is based on the principle of

integrating micro-structures on a flexible substrate. Usually, the silicon substrate is placed on a flexible substrate, for example, Polydimethylsiloxane (PDMS). This method can balance out the disadvantages of non-flexible silicon-based chips that are thick and brittle, making the electronic devices flexible and light and thin and anti-knock. From the initial "wave" structure [14, 15] to the current more stretchable buckling in serpentine microstructure, not only the max strain reaches 170%, the occupancy of the active device has also reached 81% [16]. Figure 1.2 gives the serpentine structures used in Yihui's study. At the same time, the silicon substrate is replaced by a large amount of inexpensive plastic substrates, the cost is greatly reduced. The development of flexible electronic technology will inevitably create new application areas for the design electronic products which has various shapes, fitting the human body and is easy to use, such as flexible sensors, flexible electronic eyes, wearable electronic clothing, flexible electronic paper, flexible circuit boards, artificial muscles, flexible heart monitoring clothing, flexible keyboards and flexible electronic displays. Compared with traditional electronic devices, flexible electronic devices with extraordinary flexibility and extensibility will undoubtedly have a prospect of comprehensive and practical applications in the areas of communications and information, biomedicine, machinery manufacturing, aerospace and defense security.

Apart from the broad prospect in development, flexible electronics also have very high commercial value due to its advantages of being lightweight, flexible, extensible, and adaptable to complex and uneven surfaces. Many countries have included flexible electronics research in their major national development plans. Many universities and research institutes have scrambled to join the study of flexible electronics. Many internationally well-known universities like Illinois University, Northwestern University, Princeton University, Harvard University and Cambridge University have established research institutes specifically for flexible electronic technology. Intel, IBM, Philips, Sony and other leading companies have invested a lot of manpower for related research and development.

In 2008, Prof. Y. Huang's research group [17, 18] analyzed the mechanical properties of

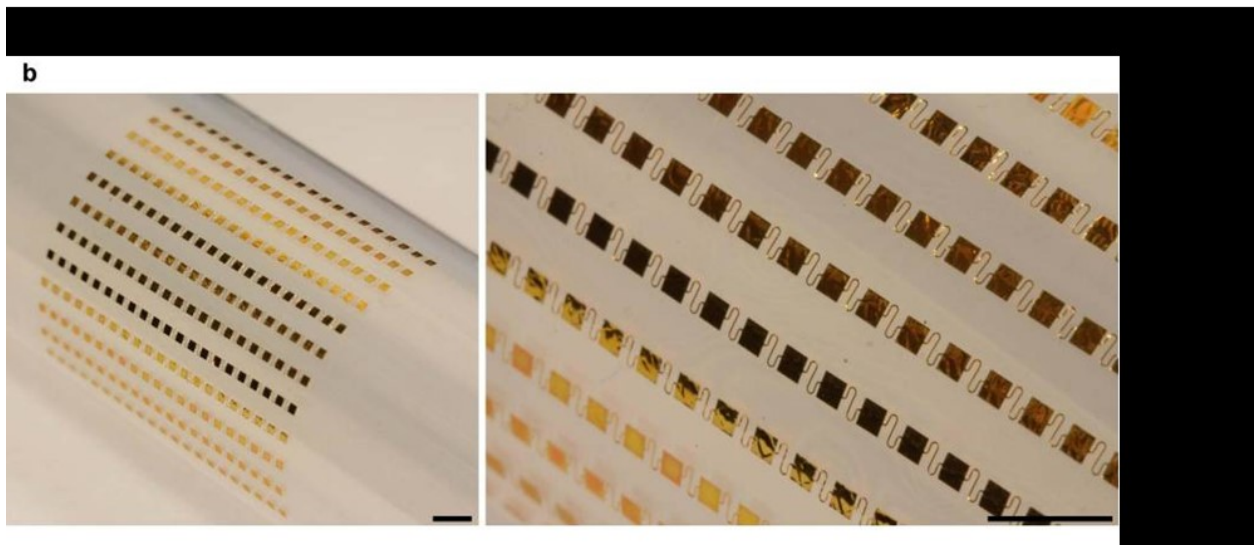
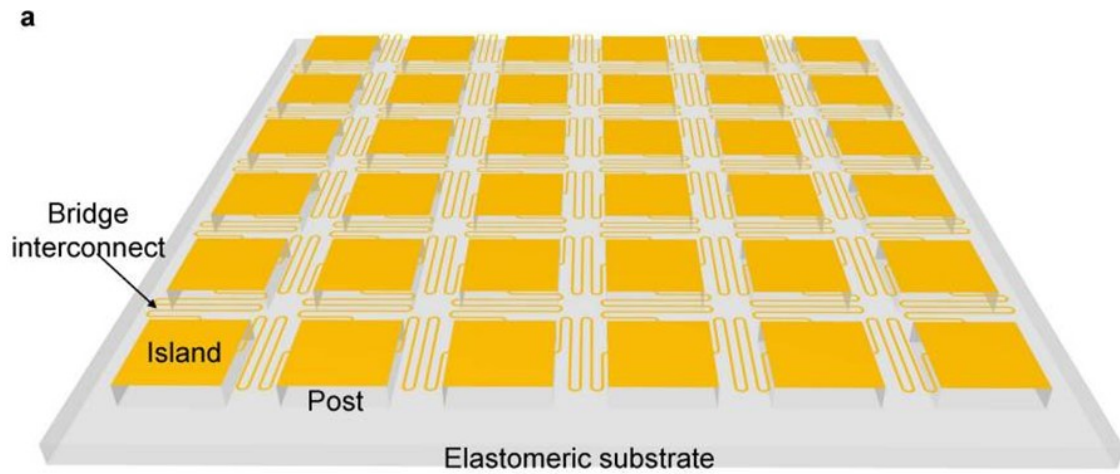


Figure 1.2 (a) Schematic of the island-bridge structure with serpentine geometry; (b) optical image of the as fabricated serpentine structures.[16]

the hard film-soft substrate compliant structure, studied the controllable buckled structure of the hard film on the flexible substrate. Meanwhile the controllable bending mechanism of thin-film nanobelts on compliant substrate was analyzed [19], and the precise control of corrugated structures was studied from the mechanical mechanism [20]. The joint team of Prof. Y. Huang and Prof. J. A. Rogers [21] successfully fabricated the world's first flexible electronic eye camera, and introduced the structure, function and preparation process of the flexible electronic eye. Figure 1.A. J. Baca et al. [22] introduced the method of combining phase shift lithography with anisotropic chemical etching. This method can be used to

produce high-quality single crystal silicon nano bars or nano thin films. A. Carlson et al. [23] studied the transfer technology for the materials assembly and devices assembly at micro-nanometer. R. Saeidpourazar et al. [24] introduced the method of micro-structure fabrication using laser driven micro-transfer placement. In 2012 Prof. J. A. Rogers [25] introduced the latest research results of nanometer-scale printing. Team of Prof. J.A Rogers [26] have done a lot of research from theoretical analysis to experimental verification and preparation. Using the printing technology to make single crystal silicon film strips integrated on a flexible plastic substrate, a flexible integrated circuit was successfully prepared. A flexible broadband membrane reflector [27] was prepared on glass and it was found that incorporation of InGaAs in silicon films of silicon solar cells can enhance cell efficiency [28], and micro and nanopatterning techniques for flexible electronics are studied [29]. Successfully fabricated microstructures on the device surface, Prof. S. Wagner [30] studied the bending and stretching properties of microelectronics, analyzed the mechanical properties of bending deformation of the structure, studied the connection of stretchable electronic circuits in flexible electronic structures [31], and analyzed the connection problem of the corrugated structure of the metal wire [32]. Prof. Z.G. Suo's research team [33] conducted research work on the thin film and interface fracture in flexible structures, analyzed the mechanical properties of the stretchable metal film on the elastic substrate, and crack initiation of the composite structure containing the organism from the dynamics [34]. J. Wu et al. [35, 36] pointed out that the flexible substrate in a flexible electronic structure has the effect of strain isolation, and the transfer printing efficiency is analyzed using a viscoelastic model [37]. J. Xiao et al. [38] conducted theoretical analysis and experimental research on the buckling mechanism of the film, studied the dynamically tunable hemispherical electronic eye camera system with adjustable zoom capability [39], and analyzed the noncoplanar design for stretchable electronic circuits and structural mechanical properties [40]. G.X. Qin et al. [41] studied the performance of flexible thin-film structures and the fabrication of flexible nanodevices. The high-frequency characteristics of flexible silicon thin-film transistors on

plastic substrates under bending conditions were analyzed, and the flexibility on plastic substrates was studied, as well as microwave single crystal germanium nanomembrane diode performance and fabrication technology [42].

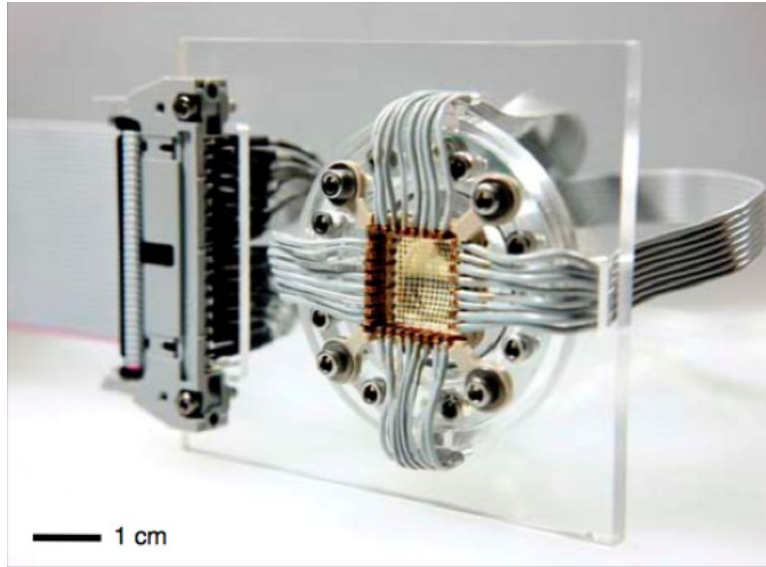


Figure 1.3 The dynamically tunable electronic eye camera from the team of John A. Rogers. [39]

The team of Z.Q. Ma [43] successfully fabricated high-speed flexible electronic devices using strained silicon thin films, fabricated large-area flexible broadband reflectors using laser interference lithography [44], and analyzed the relevant characteristics of rippled graphene and silicon thin films [45]. A thermoelectric wireless sensor for fuel monitoring [46] was prepared, and semiconductor nanomembranes technology for integrating silicon photonic devices and flexible photonic devices was introduced [47]. In 2015, Queens University of Canada has developed a new concept mobile phonepaper mobile phone, which can make telephone calls and play music like other smart phones. The difference is that it is lighter and more flexible. HP has successfully developed a flexible display that is ideally suited for future handheld devices. Figure 1.3 shows the dynamically tunable electronic eye camera from the team of John A. Rogers. Figure 1.4 presents a possible structure of paper smart phone and the flexible display exhibited on HP conference.

With more and more researchers joining the research work of flexible electronics, the

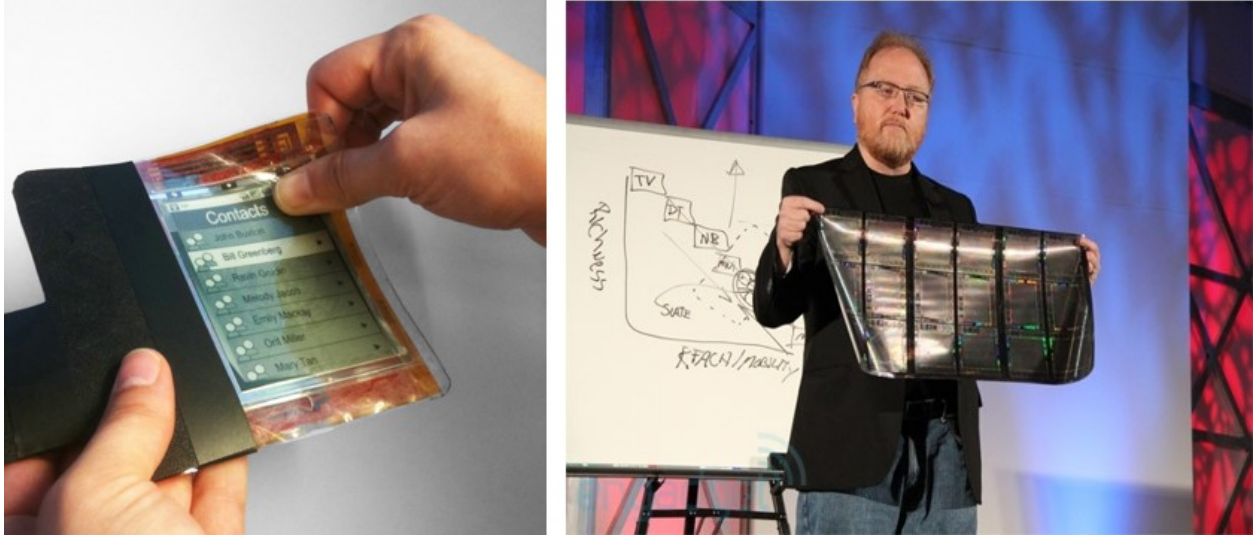


Figure 1.4 Paper smart phone and flexible display that HP exhibited in MobileBeat conference.[48] [49]

mechanical properties and performance level of flexible electronic devices will certainly be improved. In the future, more advanced materials such as carbon nanotubes, graphene, and germanium will be gradually applied to mature flexible electronic structures, and their flexibility and other properties will be greatly enhanced. New flexible sensors made with these new materials will adapt to more complex, uneven surfaces and expand the range of applications for sensors. These new flexible sensors can play an important role in electronic skin, biopharmaceuticals, wearable electronics, and aerospace, such as implantable micro-flexible temperature sensors for detection of abnormal cells in biopharmaceuticals; wearable electronic medical devices will continuously and dynamically monitor the physical condition of the human body anywhere and anytime;

Figure 1.5 shows a tattoo-like sensor that can detect glucose levels without a painful finger prick [50]. Figure 1.6 shows the study of team of Prof. Someya, they fabricated a motion sensor, thermal sensor and temperature sensor on a finger [51]. Flexible sensors can also be wrapped on the surface of the wing to monitor and transmit cruise speed and the aircraft's health information.

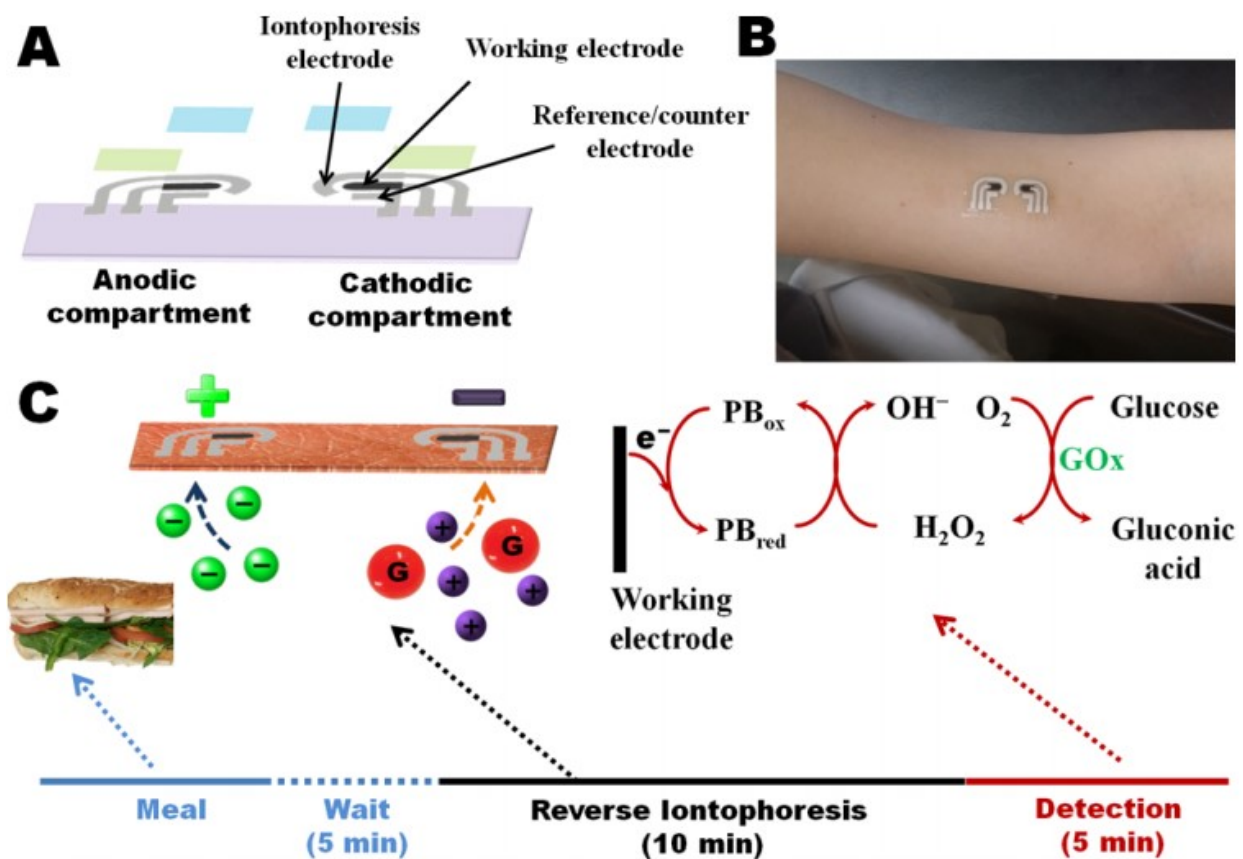


Figure 1.5 Tattoo-based platform for noninvasive glucose sensing. (A) Schematic of the printable iontophoretic-sensing system displaying the tattoo-based paper (purple), Ag/AgCl electrodes (silver), Prussian Blue electrodes (black), transparent insulating layer (green), and hydrogel layer (blue). (B) Photograph of a glucose iontophoretic-sensing tattoo device applied to a human subject. (C) Schematic of the time frame of a typical on-body study and the different processes involved in each phase.[50]

With the further development of flexible electronics research and the improvement of the manufacturing process of flexible electronic devices, it is expected that in the future people will be able to produce flexible electronic products that are more adaptable, lighter, and more economical. Paper mobile phones, flexible electronic clothing and pen-shaped flexible rollable displays will surely turn concepts into reality. In the foreseeable future, relevant flexible electronic products will be popular and greatly enriched the market. A new era, the era of flexible electronics, will surely come, and it will revolutionize electronic technology and have a major impact on human life.

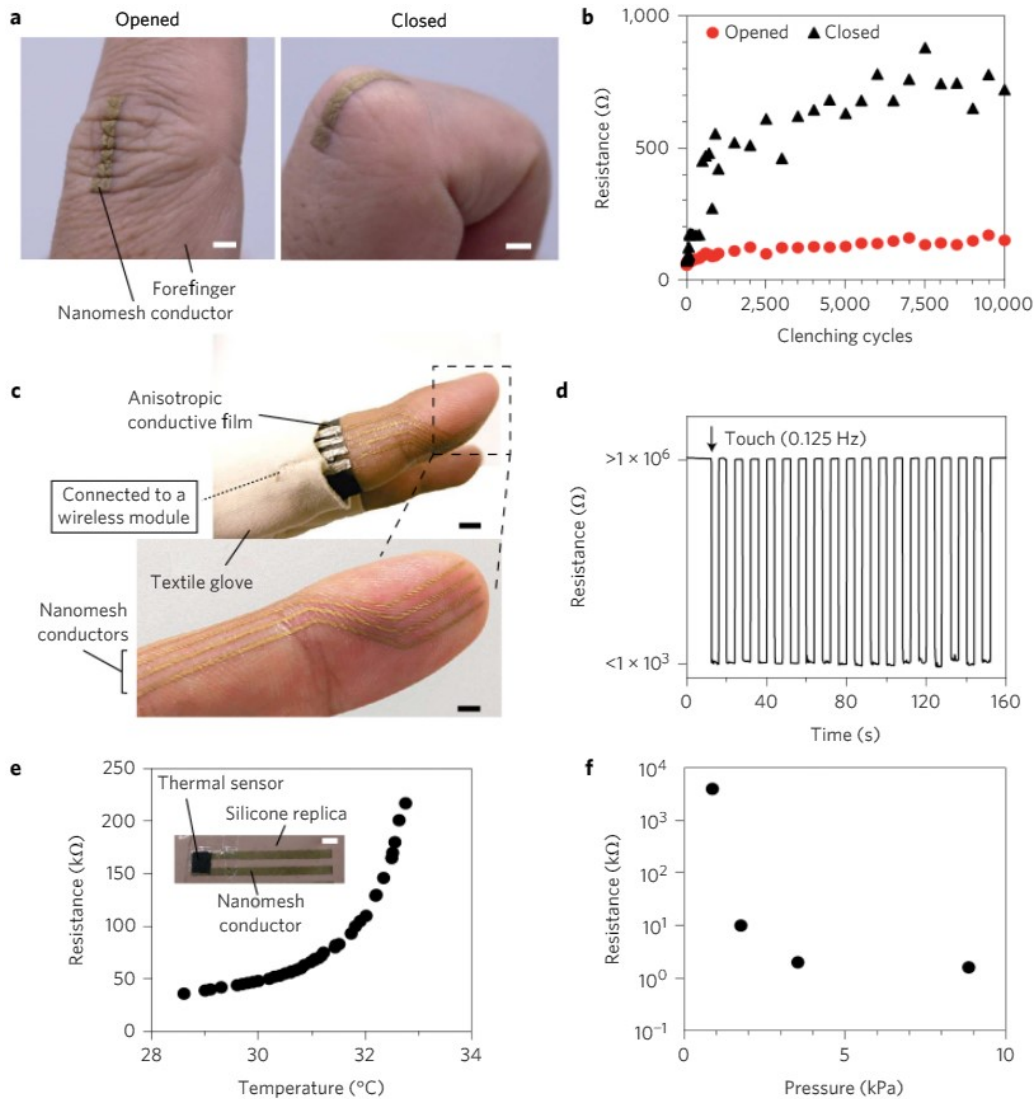


Figure 1.6 Electrical performance of nanomesh conductors on skin and their sensor applications. a, b, Conductance of nanomesh conductors attached to a finger when the hand is opened and closed. c, Depiction of an on-skin wireless sensor system. Electrical signals are transmitted from the fingertip to a wireless module through on-skin nanomesh conductors, anisotropic films and conductive threads. The electrode array acts as a touch sensor for conductive materials. It can also be used as a thermal and/or pressure sensor when polymer PTC and pressure-sensitive rubbers are attached, respectively. d-f, Electrical performance of touch (d), temperature (e) and pressure (f) sensors. The inset shown in (e) shows the thermal sensor laminated onto a silicone replica substrate with nanomesh conductors. Scale bars, 3 mm.[51]

1.1.2 Printing Method Applied in Device Fabrication

1.1.2.1 Printing Technology

Silicon-based semiconductor microelectronics technology has dominated electronics technology for half a century. However, with the development of electronic products demanding flexibility, the brittle materials used in silicon-based electronic products are insufficient in flexibility, and the production line needs a huge amount of investment and increasingly complex processes have stimulated the demand for flexible electronic technology. The research on electronic technology based on plastic substrates has developed rapidly. At this stage, there are two main manufacturing strategies for flexible electronics: One is to transfer components onto a flexible substrate by transfer printing [52]; The other is to directly fabricate components on the surface of the substrate by printing method [53]. The former is mainly based on silicon-based electronic technology, which realizes flexible circuit by transfer processing. This method still cannot resolve the complexity of the manufacturing process; the latter on the other hand is the focus of current flexible electronics development. Currently there are some published papers expounding the development of printed electronics technology, for example, Singh et al. [54] and Yin et al. [55] published inkjet printing technology. Schiff et al. [56] mainly involved nano-printing technology, Carl. Son et al. [57] published a transfer printing technique. Perl et al. [58] published an overview paper on micro contact printing, and Sndergaard et al. [59] published a roll-to-roll (R2R) processing technology paper, Khan et al. [60] reviewed the contact and non-contact printing technologies. A new electronic technology, namely printed electronics, has been created.

Table 1.1 Comparison of various fabrication technology

<i>Fabrication Technology</i>	<i>Process Steps</i>
<i>Micro – nano processing</i>	<i>Making masks – Preparing substrate – Photoresist spin coating – UV exposure – development – Etching</i>
<i>Transfer Printing</i>	<i>Preparing template – Preparing materials – Printing – Post – processing</i>
<i>Digital printing</i>	<i>Preparing materials – Printing – Post – processing</i>

Printed electronics, as the name suggests, is a process that combines traditional printing techniques to produce electronic devices. Through a variety of printing processes, pre-designed patterned structures are printed on functional inks on flexible (or non-rigid) substrates to connect electronic components [61, 62, 63, 64, 65]. The printing systems currently developed fall into two main types: contact and non-contact. In the contact process, the patterned surface with ink is used for the direct physical contact with substrate. In non-contact processes, the ink is moved through the openings or nozzles, while moving the substrate material or nozzle through a pre-programmed pattern to achieve the structure printing. Contact printing technology include gravure printing, gravure offset printing, screen printing, and elastic printing. Non-contact printing technology includes extrusion coating printing and inkjet printing. From Table 1.1, it can be seen that silicon-based microelectronics technology requires complex manufacturing processes, while printed electronics, especially digital printed electronics, greatly reduce the processing steps of circuit, and the invention of printed electronics technology has made large-scale IC and R2R production possible.

Taking traditional inkjet printing as an example, it is a method of directly printing a designed graphic structure to a substrate through a printer. It is an additive manufacturing process and is an efficient solution [66, 67, 68, 69]. Compared to the lithography process [70], digital printing electronics has unparalleled advantages. This is a crossover area integrating the two major industries of electronics and printing. Printing flexible electronic technology helps to greatly reduce the costs of fabricating electronic devices and sensors. Simple process steps, minimal material waste, low processing costs, and simple graphical techniques make

flexible electronics very attractive [71]. Among them, the key point is that digital printing does not require production of the template, which is also an important feature distinguishing it from other printing technologies. It further shortens the product's development and production cycle. At present, regardless of the printing method or the printing material, it has attracted great attention of the industry.

Flexible electronic devices require not only flexible substrates, but also to produce smaller functional circuits and components on large-area flexible substrates, and materials and substrates must have good compatibility. High-molecular organic materials [72, 73] and inorganic materials [74] are two major types of materials currently used in flexible electronics. Although high molecular organic materials can naturally combine with flexible substrate materials as they have inherent flexibility and ductility. The performance of electronic devices that are based on high molecular organic materials is not ideal. Especially its electrical conductivity often fails to meet the requirements of electronic components. This has led to attention about the use of inorganic materials for flexible electronic processing to supplement organic materials. Conductive materials made of metal nanoparticles have been widely praised [75, 76, 77, 78], but the use of non-flexible inorganic materials has encountered great challenges in the design and processing of stretchable and foldable devices. So many researchers start to optimize structure design such as the use of inorganic thin film structures, which are now widely accepted, to limit the influence that inorganic materials used in flexible electronic devices. In addition, other inorganic conductive materials, such as carbon nanotubes, graphene, etc., have also been fabricated into conductive inks [79, 80, 81] for the preparation of functional electronic components. The mechanical properties of flexible electronic systems are the important parts of the research and development and application. Major breakthroughs that have greatly advanced the development of flexible electronics have been seen in bendability, stretchability, and cracking problem [82].

Digital Printed Electronics is an Additive Manufacturing (AM) technology. Because the manufacturing process is simple and the selectivity of materials is relatively low, it can

easily explore new materials and process ways to develop new sensors and systems. For example, a series of inorganic semiconductor materials have been developed and used for the preparation of thin-membrane transistors and flexible electronic components, as well as electronic skins for enveloping the body or prosthesis [83, 84, 85, 86]. Also, digital printing technology can easily achieve industrial production of R2R, providing a convenient way for low-cost electronics. Printing electronics technology opens up new avenues for low-cost electronic processing with its unique advantages. Research in this field is slowly incorporating microelectronic technology and traditional printing techniques [87].

1.1.2.2 Printing Materials

A typical flexible electronic device mainly comprises a flexible base layer and an electrically functional material layer. The materials used for the electrically functional material layer can be divided into conductive materials, semiconducting materials and dielectric materials. For low cost, high throughput, light weight printed electronics, a large number of organic materials and inorganic materials are used to prepare the above functional materials. In addition, an important advantage of printed electronics is that it can print any functional material, such as some composite materials have dual properties, such as insulation properties, ferroelectric properties, piezoelectric properties and photosensitivity characteristics, these materials are widely used in thin film printed electronic devices. In addition, hybrid organic/inorganic materials are also widely used in printed electronic devices [88].

For ink materials, inorganic conductive materials are mainly used in deforming wires, which acts like a blood vessel that connects all parts of the body, ensure the normal operation of the entire system. Inorganic conductive materials have always been the preferred choice for conductive materials. To achieve digital printing, many metal nanoparticles are used to prepare conductive printing inks, such as gold nanoparticles, silver nanoparticles, and copper nanoparticles [89, 90]. Among metal materials, copper is relatively easily oxidized, gold is expensive, and silver has good physical and electronic properties, so all kinds

of printed materials based on metallic silver are the main choices for most researchers [91]. Carbon nanotubes (CNTs) have many excellent physical properties, such as good conductivity, good mechanical strength, selectable semiconductor/metal characteristics, and good field emission behavior. CNTs are divided into single-walled and multi-walled carbon nanotubes (SWCNTs/MWCNTs). These carbon nanotubes have a wide range of applications in many devices [92]. Carbon nanotubes, after a certain treatment, dissolved in water with dispersant are used to prepare printed conductive film materials [93, 94]. But often the first layer of printing does not have a very good conductive network. When the number of print layers increases, the conductive network gradually becomes better. Graphene has the same electrical conductivity and uniqueness as the metal conductor in the printed electronics. The advantages of these excellent properties include high conductivity, chemical stability, and flexibility, among others [95]. Seekaew et al. [96] use the combination of graphene and PEDOT:PSS to print out gas detectors. Graphene has become an emerging materials, which gets rapid development and application in printing flexible electronics.

Utilizing different printing technologies, the high-molecular polymer flexible substrate can provide a low-cost, high-speed, large-area production substrate material for the flexible electronic device. In order to replace the rigid substrate, the flexible substrate material needs to have a stable structure size, thermal stability, low coefficient of thermal expansion (CTE), very good resistance to dissolution, and good water and gas barrier properties. There are three types of base materials, thin glass, metal foil, and plastic [97, 98]. Thin glass is flexible, but its brittleness limits its use on flexible electronic devices. The metal foil can maintain a very high temperature and can provide a deposited platform for inorganic materials, but its surface roughness and high material cost affect its use on flexible electronic devices. Plastic substrate materials have high bending properties, transparency, low cost and other characteristics, so the plastic substrate material is a compromise in physical, chemical, mechanical and optical properties.

1.1.2.3 Inkjet Printing

The main printing process used in this thesis is inkjet printing. Inkjet printing is a common printing technology. Its principle is the same as our ordinary inkjet printer. It can directly print some complex 2D or 3D structure drawings from computer software. This printing technology has already begun being widely used in electronic devices, biological devices and other sensors [99, 100]. Inkjet printing is the formation of text or images by spraying conductive ink onto the substrate, which is a non-contact printing. In this way, there is no restriction on the choice of substrate material, either on the plane or on a non-planar. When the head is integrated into a multi-degree system for 3D printing.

Inkjet printing can be used to realize true 3D electronic printing. Pulse Electronics has introduced the FluidANT family of products for antenna printing, including a 3D printer called FluidWRITER that can be used to print any circuit structure on any 3D object, including curved flexible surfaces. Ink jet printing eliminates the need for masks, allowing direct use of CAD/CAM data for processing, greatly enhancing the flexibility of manufacturing. Inkjet printing has been widely recognized in the printing of flexible electronic devices [101, 102]. Except of a few organic materials, almost all electrical functional materials cannot be printed directly, so printed materials need to be made with solvents. Inkjet inks or colloidal solutions. The development of colloidal solutions has provided fundamentals for achieving droplet ejection in targeted areas. But it still faces significant challenges in order to guarantee the performance and acceptability of printed circuits. It is due to the evaporation speed of the solvent and the directivity of the active particles that will directly affect the quality of the circuit. At the same time, the ink jet printing technology is limited in resolution (2050 m or more) due to the behavioral dynamics of the droplet flying and the way to the target substrate. Therefore, when the technology is used for printing flexible electronic devices, the physical properties of the ink, the driving method of the printer, the selection of the substrate material, and the control of the printing process are all important parameters. The ink viscosity, concentration, and solvent system will directly affect the

quality and stability of printing. How to ensure continuous ejection of ink droplets without clogging the nozzle. The traditional low-speed inkjet printing process leads to low productivity, which makes the printing electronics industry production technology become very challenging. In addition, the limited number and possible blocking problems of the nozzle make inkjet printing complicated. With the application of inkjet technology in flexible electronic printing, these problems have been solved slowly. Traditional inkjet printing methods mainly use push processing methods. Through two common methods, one is piezoelectric, the other is hot bubble to eject ink. There are two more common ink-jet methods used to generate ink droplets, one is a continuous jet (CIJ). This method can generate continuous jets of uniform spacing and size through periodic disturbances. The other one is Drop On Demand (DOD), which can generate inkjet droplets as needed. No matter using which mode of printing, important physical characteristics are the surface tension and viscosity of the inkjet ink, as well as the frequency and amplitude of the modulation. Because these parameters directly affect the print quality and accuracy. In general, the CIJ system requires lower viscosity than the DOD system. At the same ink jet speed, a larger number of liquid pumps and circulatory systems are required. The DOD method is widely used due to its high precision, controllability, and high material utilization.

1.2 Contributions

In this thesis, we have developed a direct printing process for additively pattern AgNWs with length up to ~ 40 μm on various substrates. Well-defined and uniform AgNW features could be obtained by optimizing the printing conditions including nozzle size, ink formulation, surface energy, substrate temperature, and printing speed. Systematic characterizations were performed to investigate the electrical and electromechanical properties of the printed features with different nanowire lengths. By printing the AgNWs on a biaxially pre-stretched PDMS substrate, we have realized a stretchable conductor that could maintain stable conductance under an areal strain of up to 156% (256% of its original area).

Additionally, using the printed parallel AgNWs as electrodes, I have demonstrated an electroluminescent display on mechanically compliant substrates, implying the great potential of this unique additive patterning method in wearable electronics applications.

In chapter 3, I fabricated a soft, low-cost strain gauge through directly printing AgNP ink on a PUA substrate, Which can detect pressure changes with high sensitivity. The performance of this sensor is good and I can use it to sense very small pressure. Its resistance increases 100% when a 5.5 kPa pressure is applied on it. I tried to apply it on heartbeat detection and successfully get human heart rate. Also I used it in wind sensing because wind can cause little deformation on the sensor then change its resistance.

1.3 Thesis Organization

This thesis is outlined as follows: In chapter 1, the concept and characteristics of flexible electronics are introduced, and several methods for achieving flexibility of electronic devices are analyzed and compared. The development status of flexible electronic technology is reviewed. I also discussed the research progress and existing deficiencies of the flexible electronic technology. The development prospects of flexible electronic technology are analyzed and predicted. In the second half of Background part, I reviewed the application and research progress of digital printing technology based on flexible substrates, including printed materials on flexible substrates, flexible substrate materials, digital printing technologies, and digital printing applications on flexible electronic devices. Explained the limitations of traditional technologies and the advantages of digital printing flexible electronics. I analyzed the key technologies and applications of various aspects of printing flexible electronics. Introduced the inkjet printing which is mainly used in completing this thesis. Chapter 2 shows a direct printing method additively pattern AgNWs with length of up to ~ 40 m on various substrates uniformly. I discussed the test results and introduced possible its application in making sensors and display. In chapter 3, I developed a soft pressure sensor through printing AgNPs on an elastic substrate, which is very sensitive to the positive pressure applied on it.

I did a series test and discussed the results. Its expected applications on heartbeat detection and wind speed sensing are also discussed.

CHAPTER 2

DIRECT PRINTING FOR ADDITIVE PATTERNING OF SILVER NANOWIRES FOR DISPLAY APPLICATION

A unique direct printing method has been developed to additively pattern silver nanowires (AgNWs) with length of up to 40 μm . Uniform and well-defined AgNW features have been printed on various substrates by optimizing a series of parameters including ink composition, printing speed, nozzle size, substrate temperature and hydrophobicity of the substrate surface. The capability of directly printing such long AgNWs is essential for stretchable electronics applications where mechanical compliance is required, as manifested by a systematic study comparing the electrical and electromechanical performance of printed AgNW features with different nanowire lengths. Such printed AgNWs have been used to demonstrate biaxially stretchable conductors and stretchable electroluminescent displays, indicating their great potential for applications in low-cost wearable electronics. This strategy is adaptable to other material platforms like semiconducting nanowires, which may offer a cost-effective entry to various nanowire-based mechanically compliant sensory and optoelectronic systems.

2.1 Introduction

Materials with high electrical conductivity and excellent mechanical compliance are crucial to realize stretchable electronics [103]. Researchers have explored a wide range of materials, among which are carbon nanotubes [104], graphene [105], metal nanowires [106], conductive polymers [107] and metal nanoparticles dispersed in elastomers [108]. Silver nanowires (AgNWs), in particular, are considered as one of the most promising candidates owing to the combination of superior conductivity, high transparency, relatively low cost, and excellent stretchability [109]. In recent years, AgNWs have been extensively investigated as not only stretchable conductors but also electrodes of various flexible and stretchable functional devices like light emitting diodes [110], solar cells [111], and electronic skins [112]. Despite

the significant progress in the field, patterning AgNWs by additive manufacturing methods such as ink-jet printing that can significantly reduce the fabrication cost and improve the design flexibility [113] has rarely been investigated and proven extremely challenging. In most published studies, the AgNW networks were deposited by drop casting or rod coating that does not possess patterning capability unless combined with specially engineered hydrophobic/hydrophilic micropatterns to manipulate wetting of the AgNW dispersion on substrate surfaces [114]. There are several reports of patterning AgNW networks by stencil printing or spray coating through a shadow mask, albeit with patterning resolution limited to millimeter scale and inevitable material waste. Indeed, the use of masks greatly compromises the adaptability and flexibility of these methods.

The reasons that the direct printing of AgNWs can be extremely challenging are multifold [115]. Firstly, the AgNWs used as stretchable conductors are usually at least tens of micrometers long, which significantly exceeds the empirically determined printable size of $a/50$ (a is the size of the printing nozzle) for regular ink-jet printers. Hence the nozzle tends to be clogged very easily. An additional issue is the lack of effective control over the ink bleeding and solvent evaporation because of the low volume content of AgNWs in the ink. As a result, the printed AgNW features often possess rather rough edges and poor uniformity. Recently, researchers have tried reducing the nanowire length by ultrasonication scissoring [116] or tuning the ink rheology by adding polymers to facilitate direct printing [117]. Although very sharp and uniform features can be obtained, the conductivity and stretchability are greatly compromised because of the dramatically reduced nanowire length or the presence of polymer additives. Herein, we report a method for directly printing AgNWs with length up to $\sim 40 \mu\text{m}$ on a variety of substrates including silicon wafer, polyimide, glass, polydimethylsiloxane (PDMS) and 3M VHB tape. By optimizing a series of printing parameters, we were able to obtain very well-defined and uniform AgNW features that can be used as stretchable interconnections as well as electrodes for capacitive pressure sensor arrays and stretchable electroluminescent displays. This unique additive patterning method

may find applications in a wide range of nanowire-based functional stretchable electronic and optoelectronic systems.

2.2 Design and Fabrication Method

Materials: Water based silver nanowire (AgNW) dispersion was purchased from ACS Materials, LLC. PDMS (Sylgard 184) and Ecoflex (0010) were purchased from Dow Corning and Smooth-on, respectively. Ethylene glycol and Triton X-100 were purchased from Alfa Aesar and Sigma Aldrich, respectively. Liquid metal (Galinstan) and PELCO colloidal silver paste were purchased from Rotometals and Ted Pella, Inc., respectively. Orange (D611), green (D512) and blue-green (D502) phosphors were purchased from Shanghai KPT Co., Ltd. Polyimide (PI-2525) was purchased from HD Microsystems. Carbon nanotube (CNT) paste (VC101) was purchased from SouthWest NanoTechnologies.

Printing AgNWs: The water-based AgNW dispersion was first centrifuged to remove Ag particles and nanowire aggregates. 20 vol.% ethylene glycol was then added to the dispersion to tune the ink rheology and to avoid non-uniform features caused by severe coffee-ring effect of pure water. The ink was subsequently printed on pristine surface of Si wafers, glass slides or polyimide films using a Sonoplot Microplotter at a substrate temperature of 60°C. Specifically, the glass micropipette was gradually brought into contact with the substrate surface, which induced a meniscus to appear and to bridge the micropipette and the substrate. The micropipette was then moved back-and-forth along a pre-designed trajectory in a controlled manner, dragging the meniscus around and leaving some AgNWs on the surface after each pass. Generally, sufficiently conductive features can be obtained by 40 printing runs. For printing on PDMS, the surface of PDMS was treated with O₂ plasma (30W, 15 sec), and 0.01 vol.% Triton X-100 was added to the ink to tune its surface energy.

Fabricating EL displays: PDMS and phosphors were mixed thoroughly with a weight ratio of 2:1 and then casted to form thin films of 130 nm thick. AgNW lines were then printed onto both sides of the composite film to fabricate the display array. The EL display

array adopts a similar structure with the pressure sensor array. For the MSU-shaped display, AgNWs were printed with the desired pattern on one side of the PDMS/phosphor composite film, and CNT paste was painted onto the other side as the back electrode. For the EL device used for luminance measurements and stretching tests, continuous AgNW networks were blade-coated on both sides of a composite film which was then sliced into narrow strips. Coppers wires were used as the measurement leads and all devices were fully encapsulated in PDMS before testing.

2.3 Test

2.3.1 Measurement Setup

Electrical and stretchability measurements: All electrical characteristics including the I-V curve, the resistance was measured using an Agilent B1500A Semiconductor Parameter Analyzer. Scanning electron micrographs and optical micrographs were captured with a Hitachi S-4700II field emission scanning electron microscope (FESEM) and an Olympus BX51 optical microscope, respectively. The stretching tests were conducted automatically using a syringe pump (Legato 110). For EL display characterization, AC voltage was generated from a function generator (Agilent 33220A) and then amplified by a voltage amplifier (Trek 2210). All measurements were carried out under ambient conditions.

2.3.2 Experimental Results and Analysis

The printing process is illustrated in Figure 2.1. Briefly, AgNW ink is loaded into a glass micropipette by capillary force. The micropipette is then brought into contact with the substrate surface. A liquid meniscus is subsequently formed if the AgNW ink wets the substrate surface. Finally, the micropipette is moved along a predefined path back-and-forth in a controlled manner and drags the meniscus around. AgNWs are consequently deposited on the trajectory of the meniscus. Unlike conventional ink-jet printing, this direct writing process does not involve delivering discrete liquid droplets onto the substrate and

thus has no problem of uncontrollable solvent evaporation or ink bleeding. In fact, the solvent dries almost immediately after the meniscus passes. Additionally, nozzle clogging can be effectively alleviated by using micropipettes with bigger openings and expelling AgNW aggregates regularly. It is nontrivial, however, to obtain uniform and sharp printed features. A number of parameters including AgNW content, solvent composition and surface tension, nozzle size, micropipette moving speed, substrate temperature as well as the hydrophobicity of substrate surface, all need to be carefully optimized. By adjusting the above parameters, we were able to achieve optimal conditions for successfully printing uniform AgNW patterns onto various substrates, as shown in Figure 2.2a and Figure 2.2b. Figure 2.3 presents the dark field optical micrograph and SEM image of the dense AgNW network printed on Si wafer, revealing very good uniformity and well-defined sharp edges.

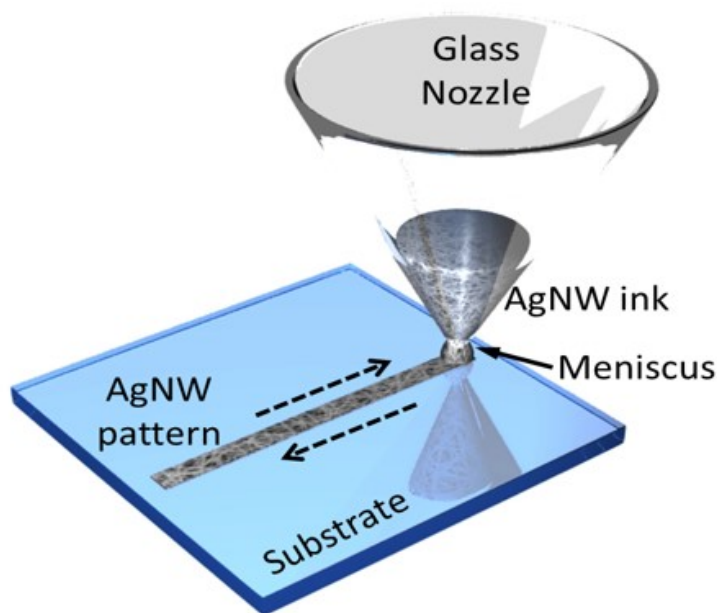


Figure 2.1 schematic diagram illustrating the printing process.[118]



Figure 2.2 (a) MSU shaped AgNW patterns printed on PDMS. Scale bar: 1 cm. (b) Straight line patterns of AgNWs printed on silicon wafer, glass slide, polyimide thin film and VHB tape. Scale bars: 2 cm.[118]

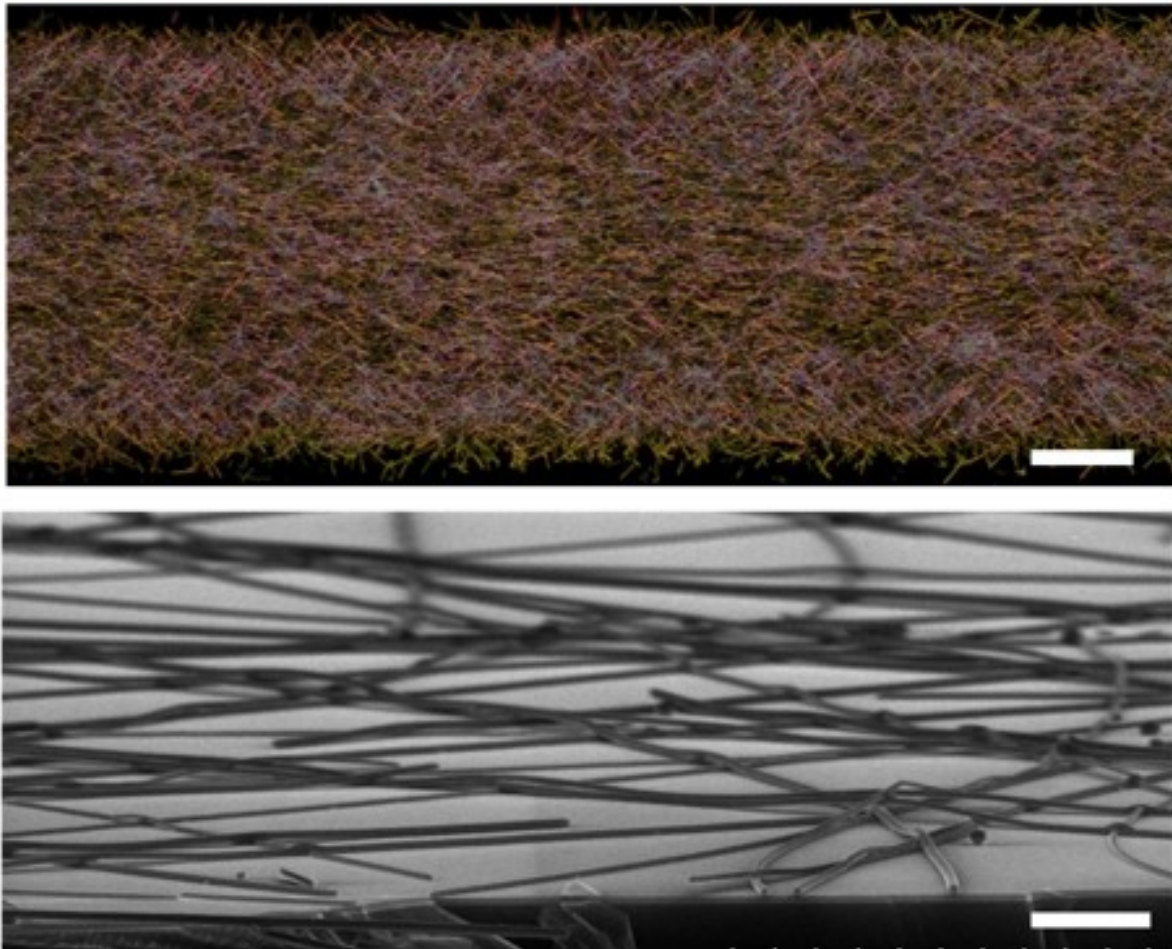


Figure 2.3 Optical micrograph (top) and SEM image (bottom) of the AgNW network printed on Si wafer. Scale bars: 50 μm and 1 μm , respectively.[118]

We have systematically studied printing of AgNW inks with different average nanowire lengths, namely 4.4 μm , 15.6 μm and 38.5 μm . Figure 2.4a and Figure 2.4b present their SEM images and nanowire length distribution, respectively. All three kinds of AgNWs can be printed with very well-defined and uniform features. It is impressive that the AgNWs with length significantly exceeding the rule-of-thumb printable size ($\approx 10 \mu\text{m}$ for typical micropipettes used here) can still be printed very easily, which is likely due to the flow-induced alignment as the nanowires pass through the nozzle. This is manifested by the well-aligned AgNWs on the inner wall of the micropipette. The electrical performance of the printed AgNW patterns, as shown below, greatly depends on the nanowire length. Figure 2.4c shows the resistance ver-

sus number of printing passes for all three kinds of AgNWs measured from printed features of 5000 m long and 500 m wide. Regardless of nanowire lengths, the feature resistance initially decreases drastically by more than an order in magnitude and starts to reduce with a much lower rate after a certain number of printing passes, implying the percolating conduction of the AgNW networks. As expected, longer nanowires require fewer printing passes to form a conductive network and have lower electrical resistance compared with patterns with shorter nanowires for a given number of passes. Figure 2.4d presents the resistance as a function of printed feature length (feature width is 500 m). All three kinds of AgNWs show excellent linearity, indicating the AgNWs are uniformly distributed throughout the entire pattern.

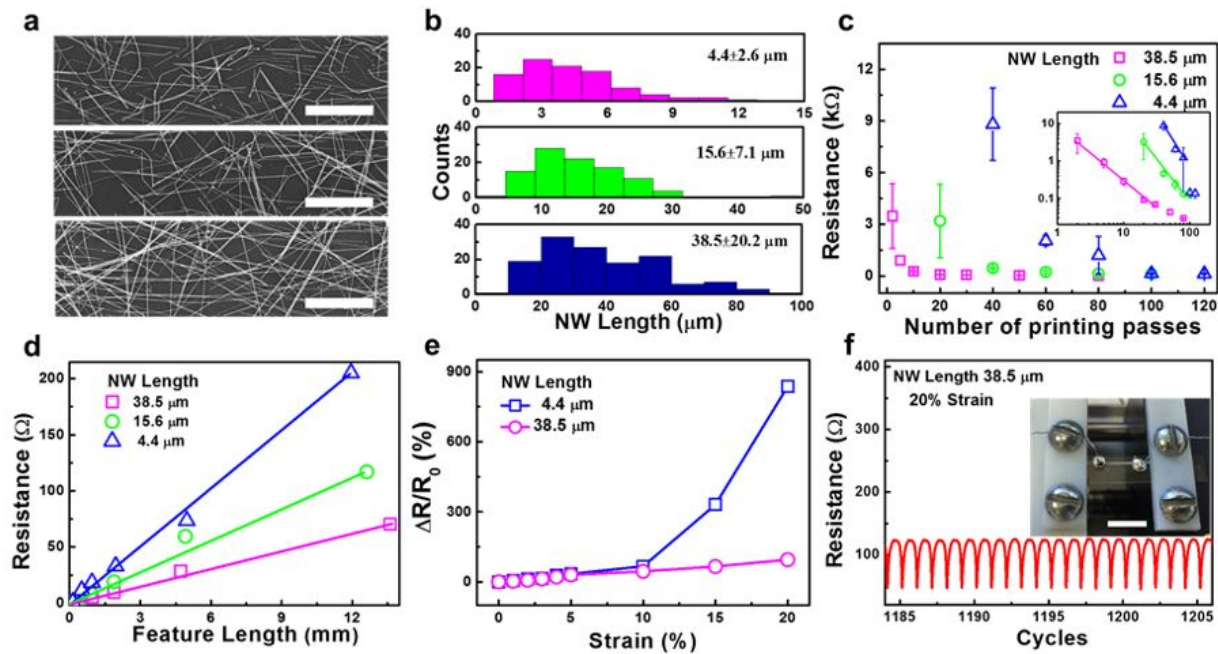


Figure 2.4 Electrical and electromechanical characterization of the printed AgNW features with different nanowire lengths. (a) SEM images of the AgNW network with average nanowire length of $\sim 4.4 \mu\text{m}$, $\sim 15.6 \mu\text{m}$ and $\sim 38.5 \mu\text{m}$ (from top to bottom). Scale bar: 5 m. (b) Nanowire length distribution of the three different AgNW inks. (c) Feature resistance as functions of number of printing runs for AgNWs with different nanowire lengths. Inset, same data presented in log scale. (d) Resistance as a function of printed feature length for all three kinds of AgNW inks. (e) Relative change in resistance as a function of tensile strain for features with average nanowire lengths of $\sim 38.5 \mu\text{m}$ and $\sim 4.4 \mu\text{m}$. (f) Cyclic stretching test results for the feature with an average nanowire length of $\sim 38.5 \mu\text{m}$. Inset, measurement setup. Scale bar: 1 cm.[118]

As mentioned above, AgNW is a promising candidate for stretchable conductors and we have found that the stretchability greatly depends on the nanowire length. Fig. 2.4e shows the stretchability of patterns printed using AgNWs with different lengths. When stretched to 20% tensile strain, the resistance of printed features with 4.4-m-long AgNWs increases drastically to nearly 10 times of its pristine value. In contrast, the resistance of features with 38.5-m-long AgNWs changes by only 90%. This difference can be interpreted by the fact that longer nanowires tend to have greater curvature and better capability to retain good inter-wire contacts upon stretching. The reliability of printed patterns with 38.5-m-long AgNWs upon cyclic stretching tests is shown in Figure 2.4f. The patterns could maintain excellent conduction at both relaxed and stretched states throughout the course of up to 2,000 stretching cycles with a maximum tensile strain of 20%.

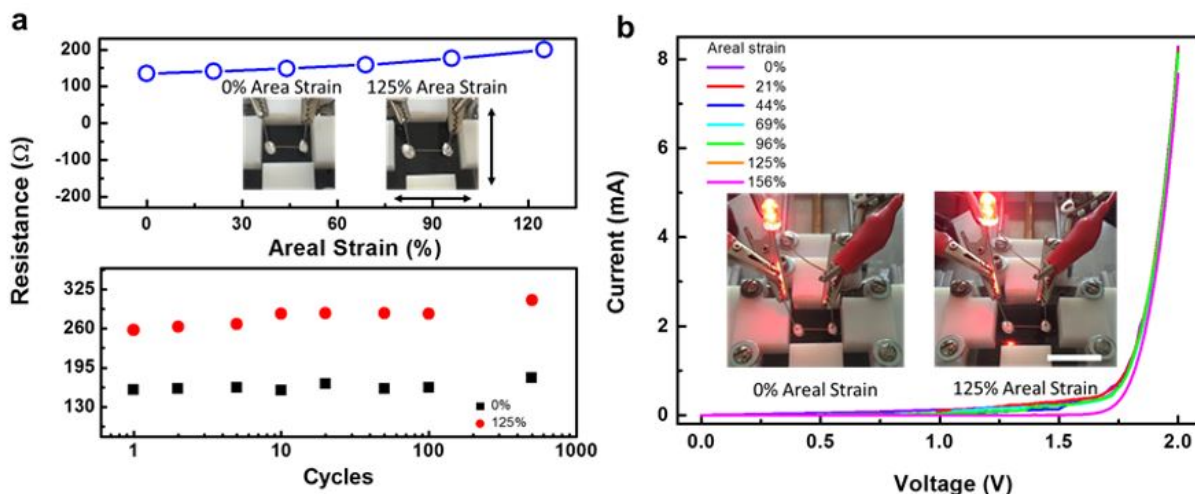


Figure 2.5 Bi-axially stretchable conductors based on the printed AgNWs. (a) Feature resistance as functions of areal tensile strain (top) and stretching cycles (bottom) for a AgNW feature printed on a bi-axially pre-stretched PDMS substrate. Insets: the sample at relaxed state (left) and being stretched to an areal strain of 125% (right). (b) The current-voltage (I-V) curves of the LED-driving circuit using the printed bi-axially stretchable AgNW conductor as interconnect with the areal strain varying from 0% to 156%. Insets: photographs of the circuit while the interconnect is under 0 (left) and 125% (right) areal tensile strain. Scale bar: 2 cm.[118]

In order to further improve the stretchability of the printed AgNW features, we pre-stretched the PDMS substrate to 30% strain along both parallel and perpendicular directions

before printing. After printing the AgNWs onto the pre-stretched PDMS substrate, the pre-applied strain was released and bi-axial stretching tests were conducted on the AgNW patterns. As shown in the top panel of Figure 2.5a, the stretchability was greatly improved by pre-stretching the substrate during the printing process. The feature resistance only increases very slightly from 145 Ω to 200 Ω when stretched to 125% areal strain (50% strain along both horizontal and vertical directions). We have also investigated the durability of the AgNW patterns printed on the pre-stretched PDMS substrates. As illustrated in the bottom panel of Figure 2.5a, the feature resistance at 0 and 125% areal strains only shows very slight change throughout the 500 stretching cycles. The application of the printed AgNW pattern as stretchable interconnection was subsequently demonstrated by incorporating it into the driving circuit of a light-emitting diode (LED). As shown in Figure 2.5b, the I-V curves of the LED essentially overlap with each other during the process of stretching the AgNW interconnect to an areal strain of 125%. Hence, the LED shows no noticeable variation in luminance, as presented in the two insets of Figure 2.5b. When the areal strain is further increased to 156%, the I-V curve shows slight downshift, but is still sufficient to drive the LED. In principle, the stretchability could potentially be improved even further by using greater pre-strains during printing. To the best of our knowledge, this is the first report of printed, bi-axially stretchable conductors based on AgNWs.

2.4 Application

The capability of direct printing offers a viable approach of additively pattern AgNWs for display applications. By sandwiching a composite composed of PDMS and electroluminescent (EL) phosphors between two AgNWs electrodes, I have demonstrated a printed stretchable EL display. It is well known that EL phosphors, like ZnS doped with transition metals, can emit light under AC voltage stimulation, which was speculated to be caused by electric field induced tunnelling through embedded junctions and subsequent radiative recombination [119]. The light intensity of the EL display increases with the magnitude and

frequency of the AC voltage. By changing the type and concentration of dopants, polychrome light emission can be realized. While EL phosphors have been widely used in the form of powder EL cells for back lighting of liquid crystal displays, they are very brittle and thus not suitable for flexible or stretchable display applications. An extensively used strategy to make stretchable materials from brittle inorganic micro-/nano- particles is to disperse them in a polymer matrix like silicone such that the desired electrical properties of the inorganic particles and the elasticity of silicone are preserved simultaneously [120]. The same strategy has proven to work well for phosphors [121]. In recent years, a couple of groups have reported stretchable EL display/lighting devices based on composites composed of silicone and phosphors. Here, I demonstrated silicone/phosphor composite-based stretchable EL displays in various configurations using our printed AgNWs as electrodes. As shown in Figure 2.6a, the EL device adopts a capacitance structure, the layer in between is a PDMS/phosphor composite. The light emission performance of the EL devices was studied systematically. Figure 2.6b presents the light emission spectra of a green EL device under various stimulation conditions. The peaks of the EL spectra center at 510 nm and show no noticeable changes when the excitation frequency changes from 0.5 kHz to 1kHz and magnitude changes from 1 kV to 2 kV. The luminance is plotted as functions of excitation frequency and magnitude in Figure 2.6c and d, respectively. As expected, the luminance increases dramatically as the excitation frequency is increased from 10 Hz to 1 kHz or as the voltage is increased from 300 V to 2 kV. The relation between luminance and excitation voltage can be fit very well using the established equation. The devices were then subjected to stretching tests and the results are shown in Figure 2.6e and f.

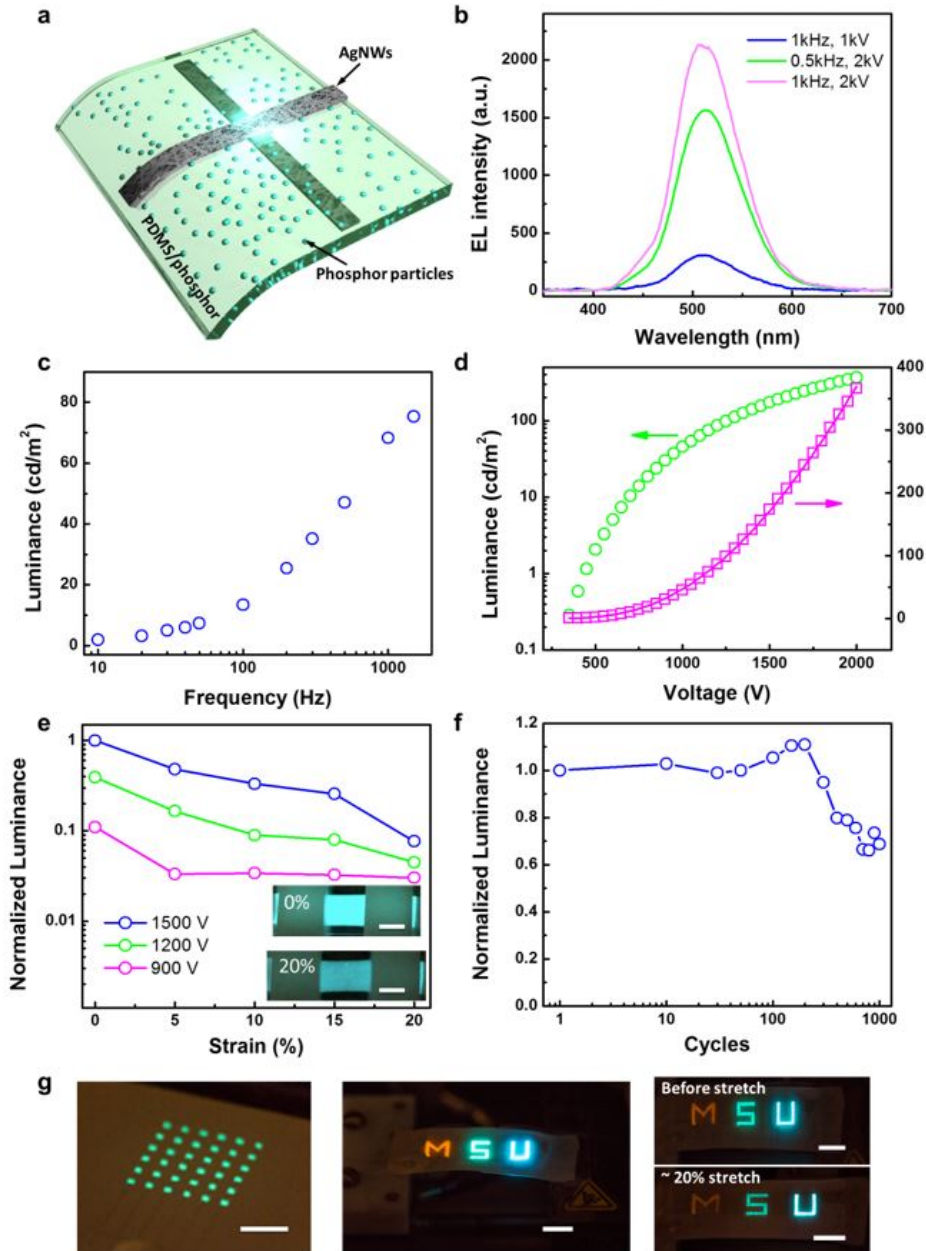


Figure 2.6 Stretchable electroluminescent (EL) displays using the printed AgNWs as electrodes. (a) Schematic of the device structure. (b) EL spectra of the device made of green phosphors under different stimulation conditions. (c, d) EL intensity of the device made of green phosphors as functions of frequency (c, measured at 1 kV) and magnitude (d, measured at 500 Hz) of the AC voltage. (e) Normalized EL intensity plotted as a function of tensile strain when measured under AC voltage with different magnitudes and a frequency of 1 kHz. Inset: photographs of a device made of green phosphors under 0 and 20% tensile strains. Scale bars: 5 mm. (f) Normalized EL intensity versus stretching cycles measured under AC voltage with a magnitude of 1.5 kV and a frequency of 1 kHz. (g) Photographs of a 6x6 EL display array made of green phosphors (left), an MSU display pattern using orange, green and blue phosphors for M, S and U, respectively (middle), and the MSU-shaped display under 0 and 20% tensile strains (right). Scale bars: 1 cm.[118]

The devices could withstand tensile strains up to 20% for more than 1000 cycles, albeit with noticeable degradation in luminance at 20% strain. The degradation in luminance could be attributed to the gradual loss in conductance of the AgNW electrodes or the electrical contacts between the electrodes and measurement leads as they get stretched. The stability in light emission performance under tensile strain can be further improved by using longer nanowires or using more robust conductive glue as the electrical contacts during the electrical measurements. Figure 2.6g presents EL display devices in different configurations that were enabled by the direct printing of AgNWs. The demonstrations include a 66 green display array (left) and an MSU shaped polychrome (orange, green and blue) display with different types of phosphors patterned in one composite film. The polychrome display worked very well under a tensile strain of 20%, albeit with some degradation in light intensity.

2.5 Conclusion

In summary, we have developed a direct printing process for additively pattern AgNWs with length up to 40 μ m on various substrates. Well-defined and uniform AgNW features could be obtained by optimizing the printing conditions including nozzle size, ink formulation, surface energy, substrate temperature, and printing speed. Systematic characterizations were performed to investigate the electrical and electromechanical properties of the printed features with different nanowire lengths. By printing the AgNWs on a biaxially pre-stretched PDMS substrate, we have realized a stretchable conductor that could maintain stable conductance under an areal strain of up to 156% (256% of its original area). Additionally, using the printed parallel AgNWs as electrodes, we have demonstrated an electroluminescent display on mechanically compliant substrates, implying the great potential of this unique additive patterning method in wearable electronics applications. Furthermore, the same strategy can be adapted to other material platforms like semiconducting nanowires, which may offer a cost-effective entry to various nanowire-based mechanically compliant sensory and optoelectronic systems.

CHAPTER 3

INKJET-PRINTED STRAIN SENSOR FOR PRESSURE SENSING

In this chapter, I studied an inkjet-printed flexible pressure sensor. I printed the silver nanoparticle ink directly on an elastic substrate. When it is subjected to longitudinal pressure, cracks will occur and the insufficient stretchability of the silver nanoparticles will influence the conductivity of wires. Thus, the change in pressure is sensed by measuring the change in resistance. The flexible substrate ensures that the device that receives pressure can be restored to its original shape after the pressure has been withdrawn. Since cracks are generated during longitudinal compression, the resistance after recovery almost has no shifts, which ensures the repeatability and stability of the sensor. From the test results, it can be seen that this type of pressure sensor has a very high sensitivity in the low-pressure section, and the sensitivity can reach around 20%/kPa. Finally, I also explored possible applications of this device in heart rate detection and wind detection.

3.1 Introduction

Among various types of sensors, pressure sensors possess the advantages of small size, light weight, high sensitivity, stability, reliability, low cost, and ease of integration. They can be widely used in measurement and control of pressure, height, acceleration, liquid flow, flow rate and liquid level. While soft flexible pressure sensors, as one of the vital component units in the next generation of wearable electronics for electronic skin [122, 123, 124, 125, 126, 127, 128], touch-on flexible displays [129, 130], soft robotics[131, 132] and energy harvesting [133, ?, 134], have drawn increasing attention. Existing soft pressure sensors are mainly based on force-induced changes in capacitance [123, 129, 135, 136], piezoelectricity [137, 138, 139], triboelectricity [128, 140] and resistivity [141, 142].

Recently, various nanomaterials, including nanowires [125, 143, 144], carbon nanotubes [129, 135, 141], polymer nanofibers [137, 139, 142, 145], metal nanoparticles [146, 147, 148]

and graphene have been used for the design of novel flexible pressure and strain sensors. The majority of these nanomaterials-based pressure sensors are based on capacitance or piezoelectricity except for a few recent reports [141, 142], where resistivity was used for designing strain gauge sensors. The advantage of resistive pressure sensors lies at simplicity in device fabrication as well as relatively low energy consumption in operation. Despite the promise, to date, only limited examples have reported success on resistivity-based flexible pressure sensors [141, 142, 149]. Metal materials that are typically used are gold, gold nanoparticles (AuNPs) and gold nanowires (AuNWs). An AuNWs based pressure sensor with low response time (less than 0.05s) has been reported [149].

AgNPs [150] has excellent electrical conductivity, as an attractive novel electronic material for flexible device fabrication. Compared with gold materials, AgNPs costs much less on material and fabrication process. The AuNWs and AuNPs based pressure sensors mentioned above are all directly depositing or coating Au NWs or AuNPs solutions on patterned substrate, most materials are wasted during this process. Herein, I developed an inkjet-printed pressure sensor fabricated by AgNPs. The device shows high sensitivity on pressure sensing and repeatability, following by two potential applications- to detect human heart rate or wind speed.

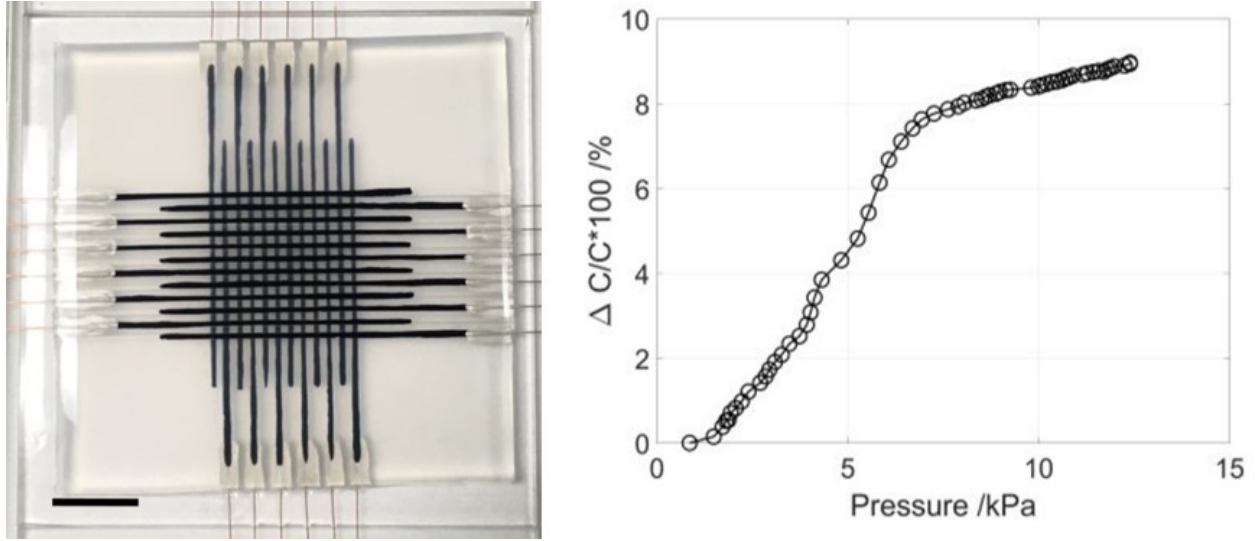


Figure 3.1 Capacitive soft pressure sensor array based on PEDOT:PSS (scale bar, 20 mm). (a) Device structure. (b) Capacitance change in response to pressure.[151]

Some capacitive soft pressure sensors have been studied. Figure 3.1a is a sandwich structure which is mostly followed [151]. A soft substrate works as dielectric layer. When pressure is applied, it reduces the thickness of the dielectric layer thereby increasing the capacitance. But the sensitive region is limited and the sensitivity is basically around 1%/kPa-5%/kPa. Figure 3.1b shows the sensitivity of the capacitive pressure sensor developed by H. Yang [151]. The pressure sensor studied in this thesis is resistive sensing. Pressure will partly break the connection between nanoparticles, cause cracks and result in a larger resistance. The AgNPs path is like a 2D structure thus the breaks along vertical direction will strongly influence the device resistance. So a higher sensitivity is obtained.

3.2 Design and Fabrication Method

Substrate preparation: The PUA substrate was made by the mixture of Siliconized urethane acrylate oligomer (CN990, Sartomer), ethoxylated bisphenol A dimethacrylate (SR540, Sartomer) and 2,2-Dimethoxy-2- phenylacetophenone (photoinitiator, Sigma-Aldrich) with the ratio of 10:1:0.01, followed by 20-mins UV light curing. The CN990 was chosen in order to improve the stretchability of the substrate, the SR540 was chosen to adjust the stiness of

the substrate and the photoinitiator serves as catalyzer.

Device fabrication: The silver nanoparticles ink (PG-007AA from Paru Corporation, South Korea) was printed onto PUA substrate (pre-treated by the oxygen plasma, 60W for 10s) using a GIX Microplotter (Sonoplot Inc.) with the layout pre-designed by the software, and then the whole device was put on top of a hotplate to be annealed for 1 hour under 120 C. Silver Conductive Epoxy Adhesive A and B (MG Chemicals Ltd) and copper wire was put on the two ends of the devices serving as the connection for measurement, and then another layer of PUA solution was poured and cured by the UV light to form the encapsulation.

3.3 Experimental Results and Analysis

The resistance was measured using an Agilent B1500A Semiconductor Parameter Analyzer. Optical micrographs were captured with an Olympus BX51 optical microscope. The pressure was automatically applied using a converted syringe pump (Legato 110). All measurements were carried out under ambient conditions.

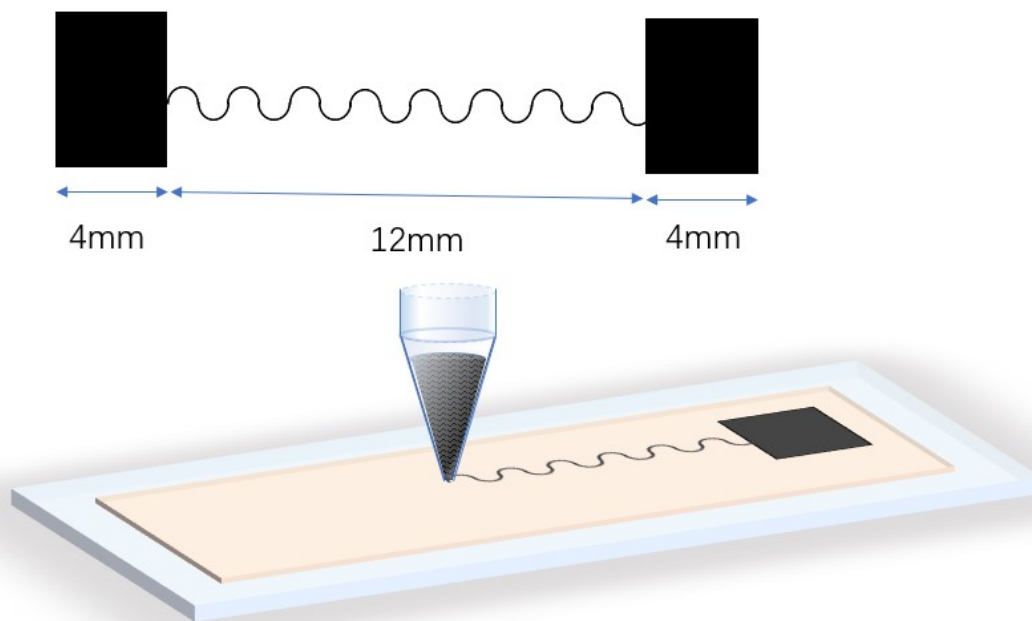


Figure 3.2 Schematic diagram of printing process and device pattern.

Figure 3.2 presents the schematic diagram of the sensor. The silver nanoparticle ink (PG-

007AA from Paru Corporation, South Korea), loaded into the ink dispenser, was printed onto a polyurethane acrylate (PUA) substrate using a GIX Microplotter (Sonoplot Inc.). To make the device stretchable, the serpentine structure was pre-designed using the SonoDraw (Sonoplot Inc.). And then the Ag pattern together with the PUA substrate was placed on a hotplate under 120 C for 1 hour to improve their conductivity. For the measurement, I have also made lead wires which are connected to the electrodes of sensors. Silver Conductive Epoxy Adhesive A and B (MG Chemicals Ltd) were combined with the ratio of 1:1. Put that combination and copper wires on the electrodes area of the sensor, waiting 30 min for drying. Then I poured another layer of PUA solution and cured it by the UV light to form the encapsulation. A finished device is presented on Figure 3.3.

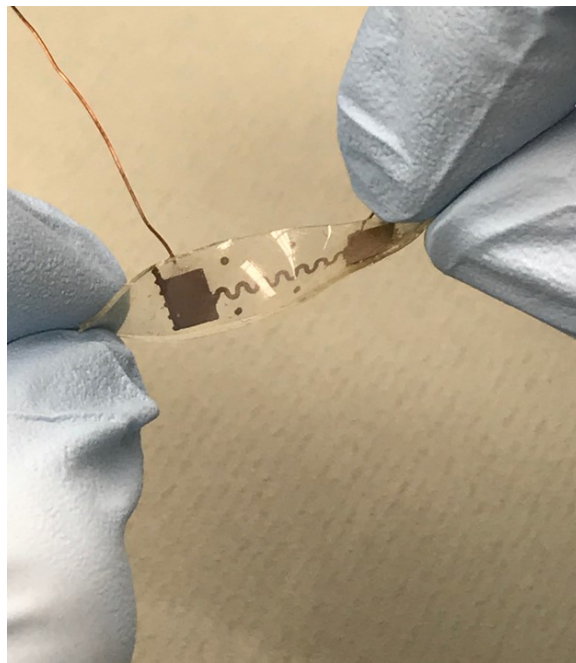


Figure 3.3 A sample of printed pressure sensor.

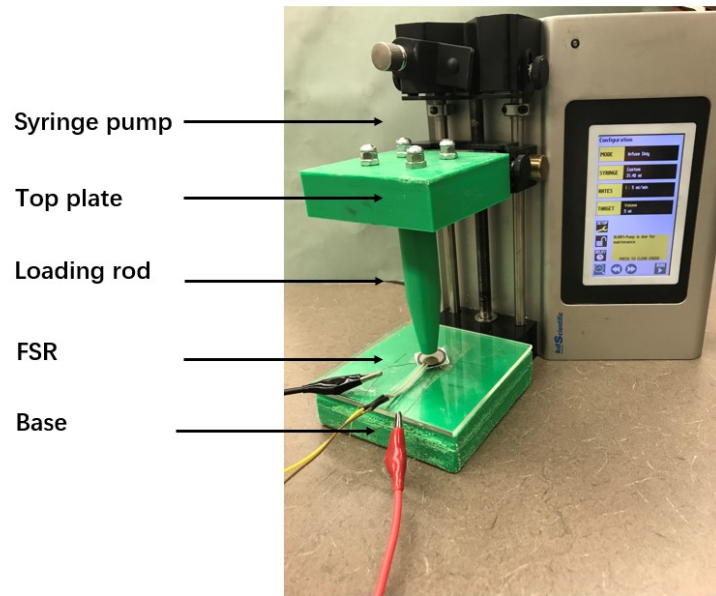


Figure 3.4 Pressure loading platform for measurement.

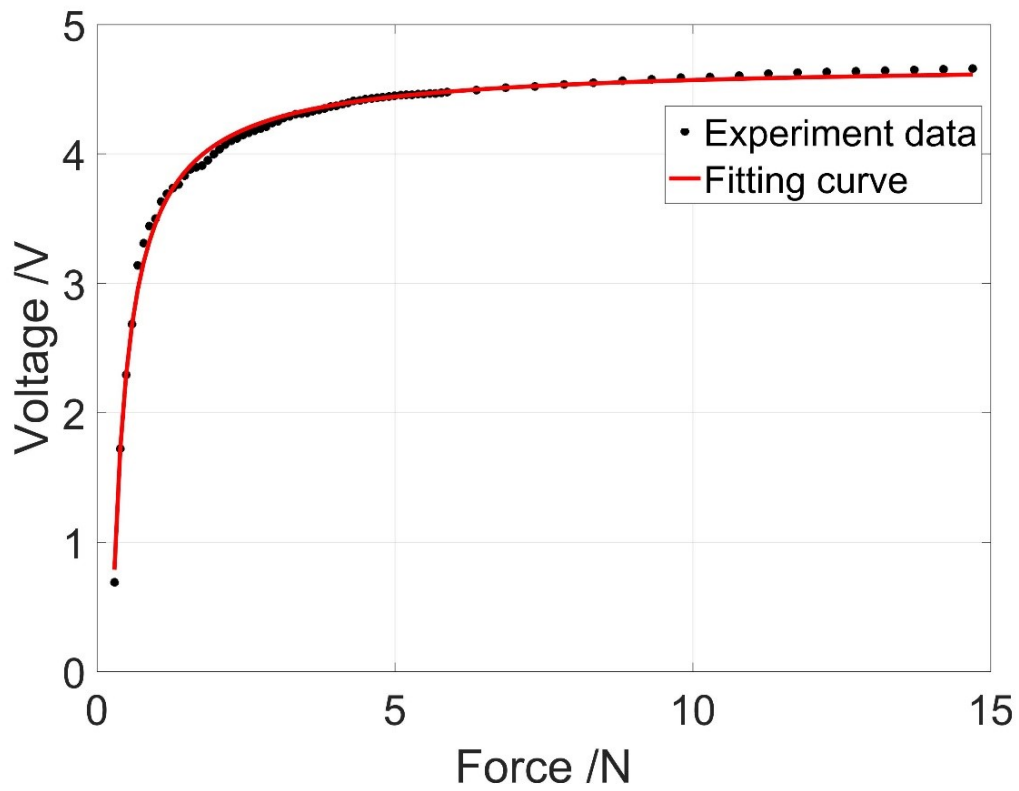


Figure 3.5 Force-to-voltage response curve of the FSR.[151]

I used a syringe pump (Legato 110, KD Scientific, Inc.) to apply the loading, through 3D-printed PLA (Polylactic acid) parts. In particular, the loading assembly consisted of three parts, a base, a loading rod, and a top plate (Figure 3.4). The loading rod was mounted on the top plate, while the base and the top plate were respectively mounted on the fixed block and pusher block of the syringe pump. To apply vertical loading, the syringe pump was placed on its side. I controlled the loading pressure by setting the displacement of the tapered loading rod. Besides, the syringe pump provided the Withdraw and Infuse mode, which enabled cyclic loading. To measure the actual pressure between the loading rod and the soft capacitive sensor, a force sensing resistor (FSR) sensor (FSR 402, Interlink Electronics, Inc.) was placed on the loading platform. I characterized the FSR device first and obtained the force-to-voltage response curve (Figure 3.5). For simplified calculation of intensity of pressure, I needed to define a constant contact area. So the FSR was attached on a glass slide (96.5 mm²), which was then placed between the loading rod and the capacitive sensor. The active area of the FSR sensor was 14.68 mm, while the loading area of the loading rod was 10 mm. When the loading rod was pressed against the soft capacitive sensor, the loading surface of the loading rod was fully covered by the FSRs active area, and the force measurement from the FSR was used to calculate the pressure applied to the sensor.

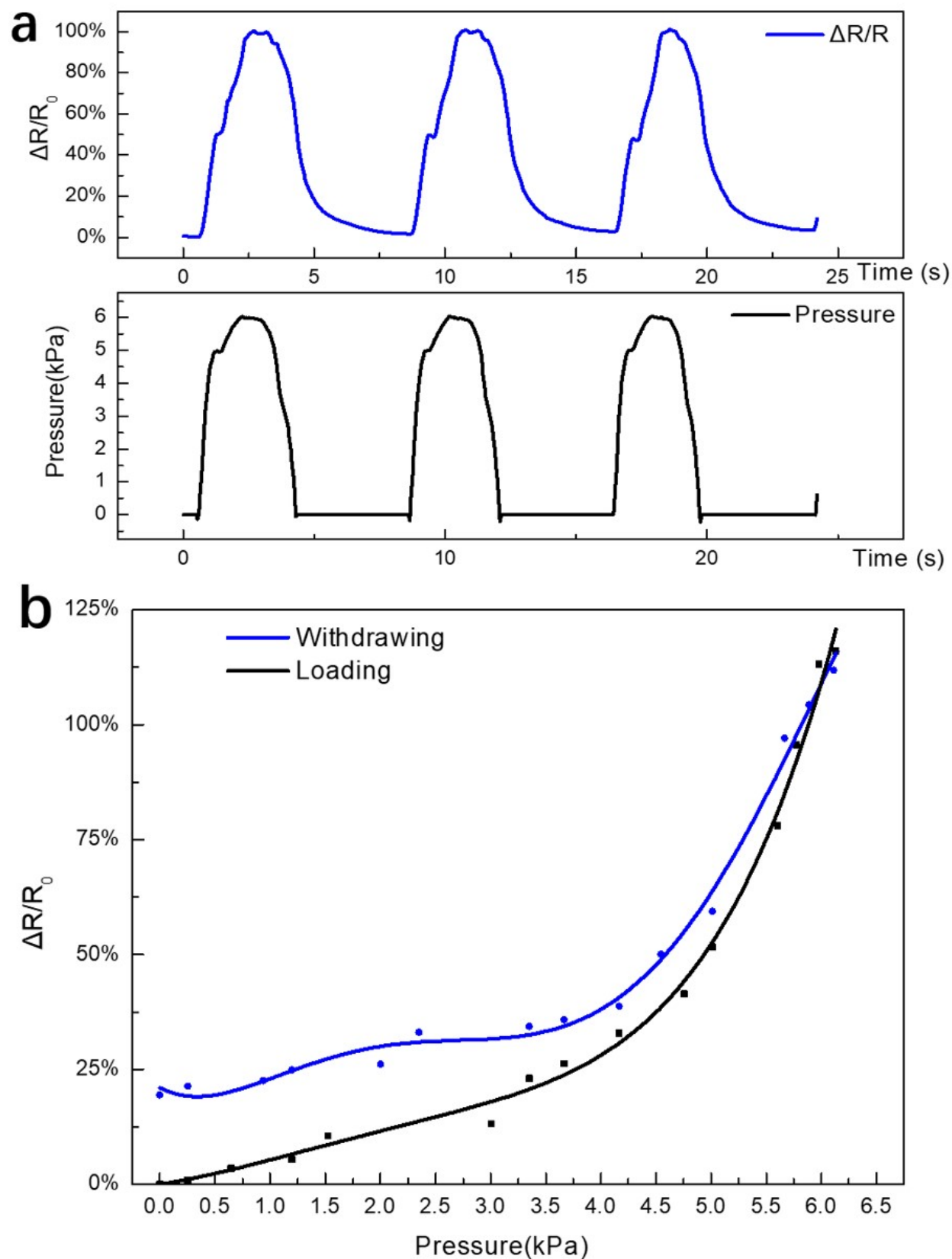


Figure 3.6 Pressure sensor based on printed AgNPs. (a) Relative change in resistance and pressure as a function of time. (b) Relative change in resistance as a function of pressure.

At first, I measured the pressure and the relative change of AgNPs pattern resistance, and the real-time record is shown in Figure 3.6a. Originally the data from FSR were voltage data, and I made a real-time conversion from voltage to intensity of pressure through Matlab. I setup the pressure loading period as 8s. From Figure 3.6a we can see that the resistance of AgNPs was changing following the pressure with an acceptable response time. The relative change in resistance can reach 19%/kPa. Also we can find difference on negative edges of the two curves, which can be found in Figure 3.6b as well. When pressure was withdrawn, the changes of resistance cannot follow the path through when pressure was applied. This is due to the recovery time of PUA substrate. The depression on the negative edge of blue curve in Figure 3.6a demonstrates that resistance cannot go back to its original value because the PUA substrate still needs about 4 more seconds to recover from deformation while at that time the pressure has already evacuated.

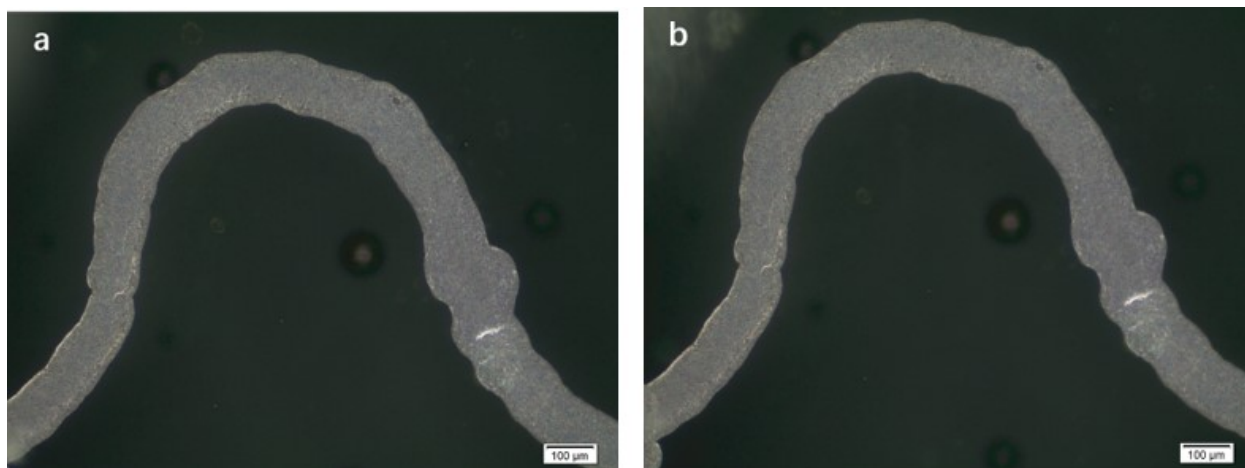


Figure 3.7 (a) Optical image of the device before test (b) Optical image of the device after test.

Since pressure was applied to the device from the longitudinal direction, it does not pull it laterally. When the pressure was removed, cracks created when the pressure is applied can be almost completely repaired as long as the substrate is given enough time. Figure 3.7 shows a sample before and after a round of test. The pattern shows almost no visible cracks under a 50x microscope. The stability and repeatability of this sensor can also be derived

from the fact that the resistance eventually returns to R_0 .

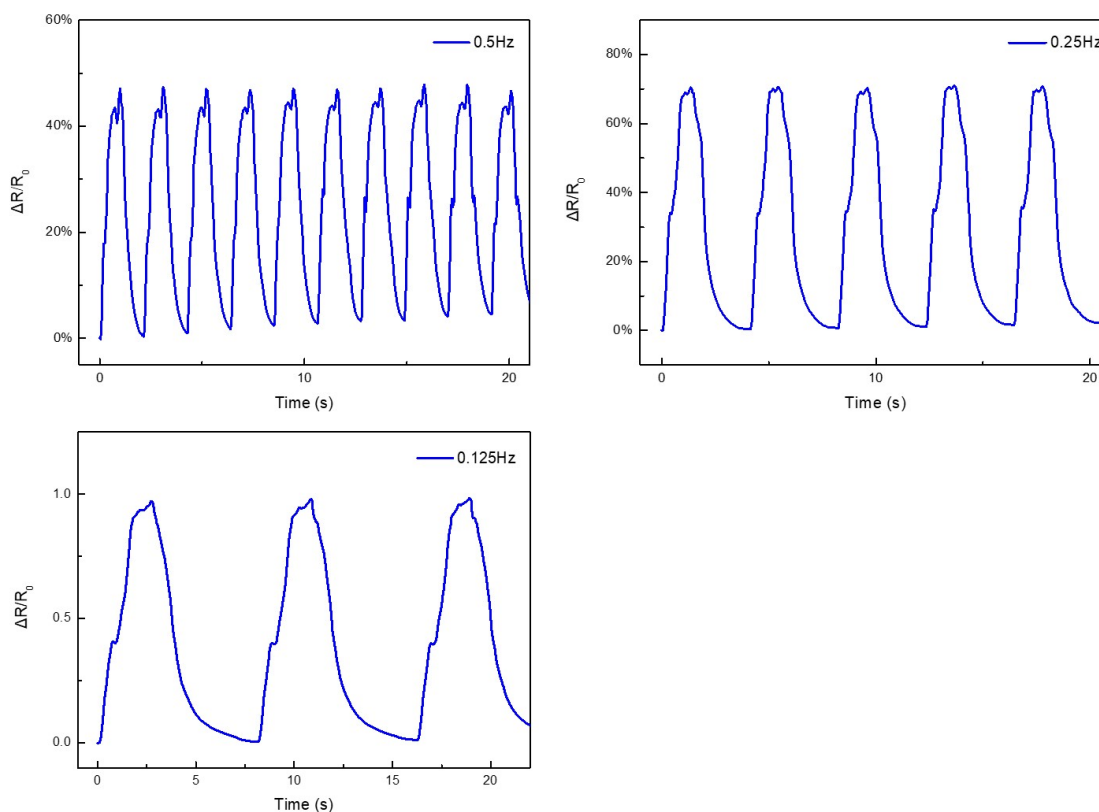


Figure 3.8 The relative change in AgNPs patterns resistance under different pressure loading frequency.

I also measured the relative change in AgNPs patterns resistance under different pressure loading frequency, as shown in Figure 3.8. Due to the defect of syringe pump, the loading rod was almost impossible go back to a constant height after all the test rounds. So the max pressure loaded in each test round varies from one to another. From Figure 3.8, we can find that the device can well adapt to pressure changes at different frequencies while high sensitivity is ensured.

3.4 Application

Flexible pressure sensors play an important role in the fields of electronic skin, artificial limbs, and medical monitoring and diagnosis. I tried to use the pressure sensor developed in

this thesis to detect heart rate and wind speed respectively.

3.4.1 Heart Rate Detection

Today's contactless heart rate sensors are mostly photoelectric sensors that use infrared or visible light for feedback. Problem is that they still have to be attached to slightly cumbersome carriers such as watches and wristbands. There are also applications that use a cell phone flash for photodetection to calculate the heart rate. However, real-time monitoring cannot be conducted in this way. Contact heart rate detectors mostly adhere to the principle of piezo-electricity, and rigid devices that are in close contact with human skin are accompanied by a user-unfriendly experience. The flexible pressure sensor in this chapter can effectuate real-time heart rate detection, and its small, soft features can better fit the appeal of comfort, having good application prospects.

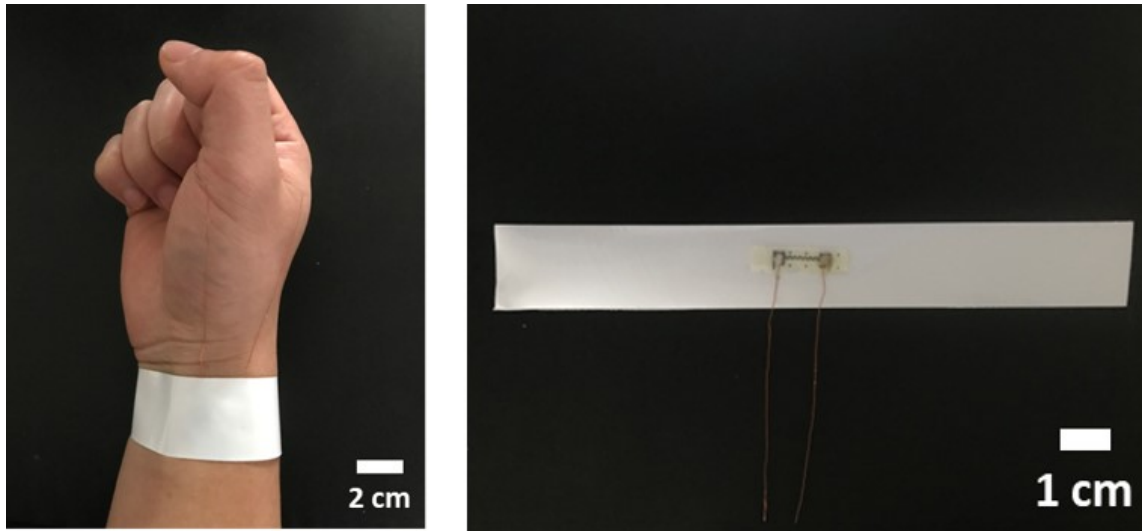


Figure 3.9 Heart rate sensing test.

Figure 3.9 shows the measurement setup for heart rate detection. The pressure sensor is simply fastened to the wrist by a cleanroom tape. In the future, other viscous materials can be used instead of tape to attach the sensor to the wrist. Pulse-induced slight deformation of the skin can be detected by the pressure sensor and fed back by changes in resistance. I

use the Agilent B1500A Semiconductor Parameter Analyzer to collect data on the resistance of the sensor as a function time.

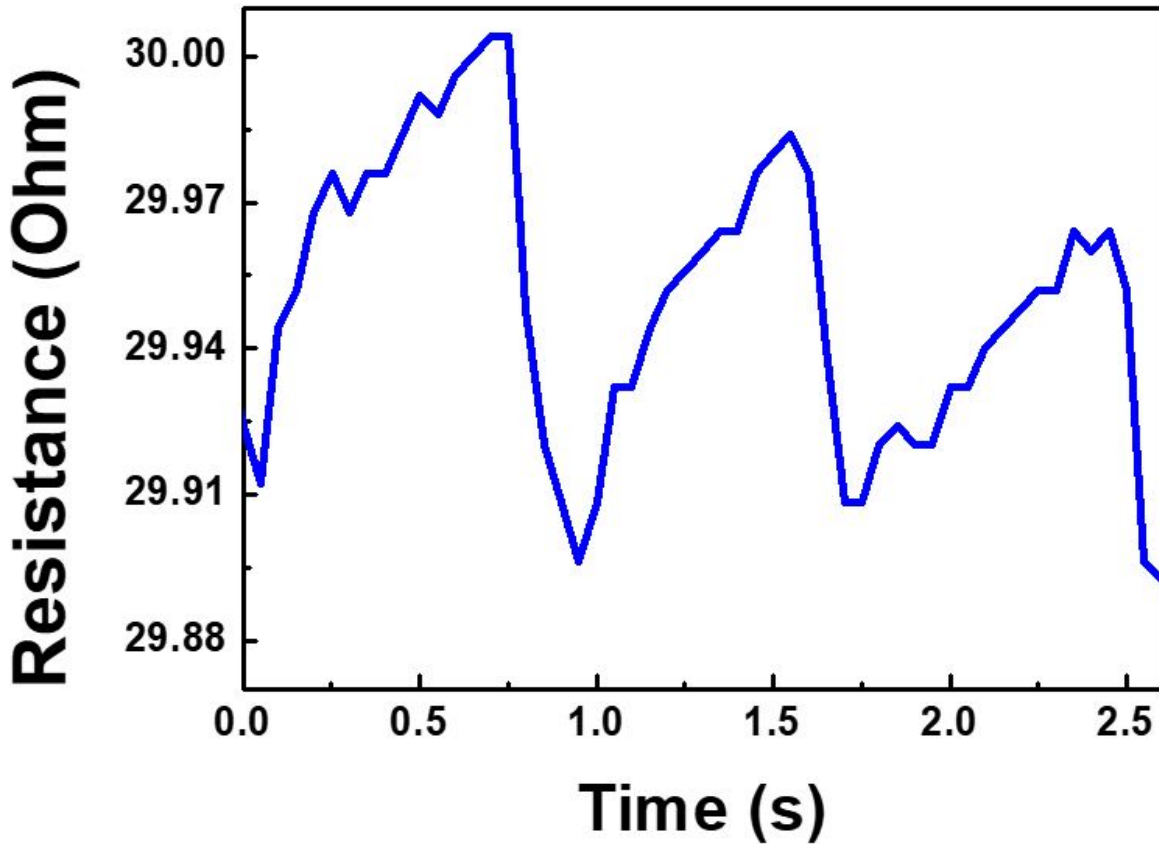


Figure 3.10 Heart rate sensing: resistance of sensor as a function of time.

Test result is presented in Figure 3.10, since the balance point of this curve kept shifting, it is hard to define where the original resistance value is. Motions of hand may cause the volatility of mean pressure. Despite the fact that original resistance kept changing, we can still get the information of heart rate as we wish. There peaks were indicated in 2.5s, so the heart rate was around 72 bpm in that test.

3.4.2 Wind Sensing

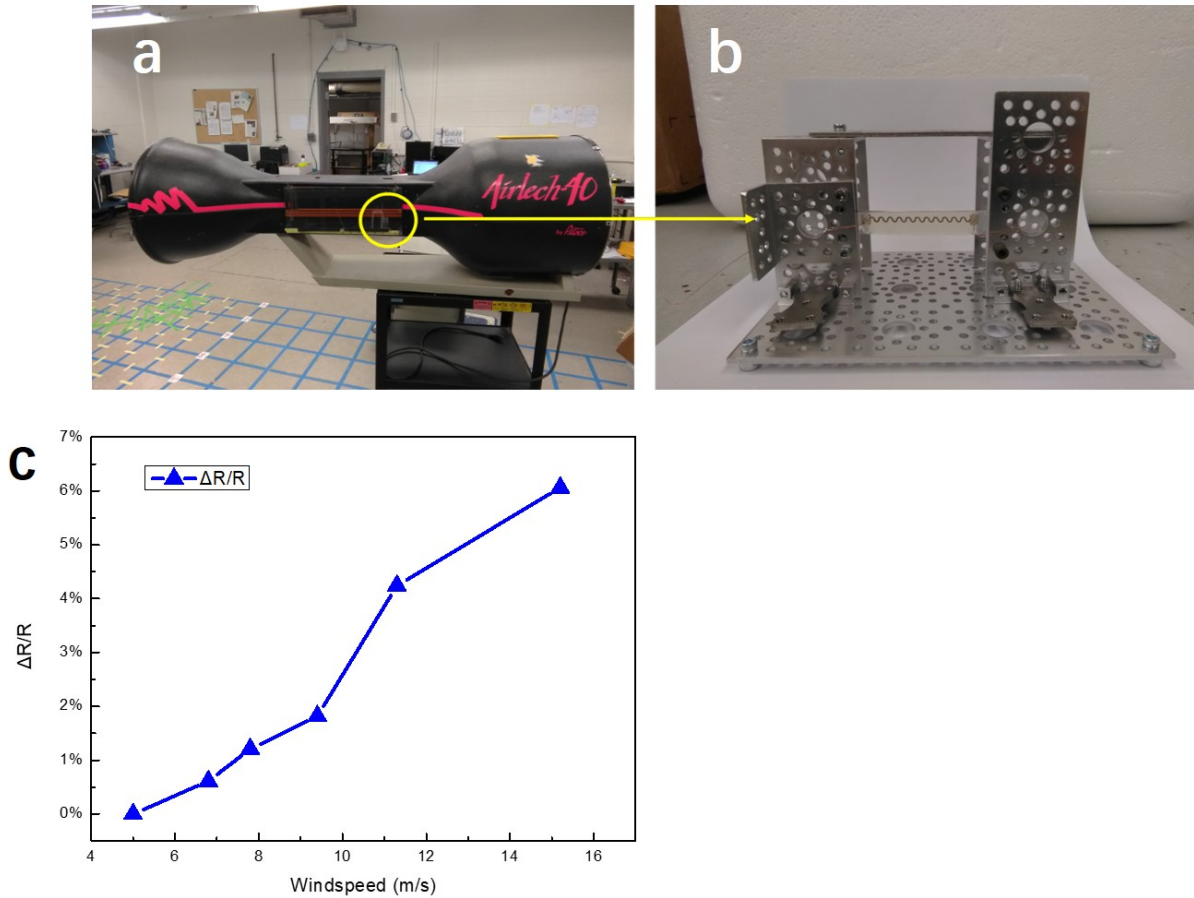


Figure 3.11 Windspeed sensing test. (a) Measurement setup. (b) Fixture for sample in wind tunnel. (c) Relative change in sensor resistance as a function of windspeed.

Due to high sensitivity of this pressure sensor, I came up with the idea of applying it to wind speed sensing. In Figure 3.11a, the sample was held in a wind tunnel by a steel frame and placed perpendicular to the wind direction. When wind blows from front of the sensor it bends the sensor, which triggers a deformation that affects the resistance. Figure 3.11c shows the result of wind sensing test. With the relative change obviously in resistance increasing by the wind speed, we are confident to see the successful application of this sensor in wind sensing.

3.5 Conclusion

In summary, I have successfully developed an inkjet-printed stretch sensor for pressure sensing by printing AgNPs ink on an elastic PUA substrate. The sensor has very high sensitivity (up to 20%/kPa) and good stability. Its flexibility allows it to fit some irregular surface like human skin, thus making happen a variety of applications. In this study I developed it for pressure sensing, heart rate detection and wind sensing. It shows consistently good performance during every test. It can be expected that this sensor will be beneficial to the research of motion detection, medical monitoring and wearable electronics.

CHAPTER 4

SUMMARY AND FUTURE WORK

4.1 Summary

Looking back at this thesis, we have developed a direct printing process for additively pattern AgNWs with length up to 40 μm on various substrates. Well-defined and uniform AgNWs features could be obtained by optimizing the printing conditions including nozzle size, ink formulation, surface energy, substrate temperature, and printing speed. Using printing technology, we have brought to fruition a stretchable conductor that could maintain stable conductance under an areal strain of up to 156% (256% of its original area) and an electroluminescent display on mechanically compliant substrates. By printing AgNPs on PUA substrate, I have demonstrated a stretchable pressure sensor with very high sensitivity which can be used for heart rate and windspeed sensing.

However, there are still some improvement should be done to the strain sensor. First, as the test platform for the pressure sensor is remolded from a syringe pump, the movement speed of the loading rod is not constant (In Figure 3.5a, the pressure curve cannot run smoothly) and it cannot memorize the original position in each test round (the max pressure is not constant in every test). Thus I missed some performance data of the sensor such as the response time and the linearity in sensitivity, which will be the priority of our subsequent work.

4.2 Future work

Whether stretchable conductor, flexible display or stretchable pressure sensor, what I made are all theoretical samples and they are far away from practical application. For flexible display, the pixels on our sample can only be lit at the same time or turned off at the same time. I cannot selectively light a certain pixel. In the future, I will add more printed

devices such as flexible resistors and flexible transistors on the samples to form circuits, and then really fulfill its function as a screen. For stretchable pressure sensor, instead of heart rate detection, our goal at the beginning of this study was to improve the existing cumbersome procedures of blood pressure measuring and achieve real-time blood pressure monitoring. The reason why I shifted our focus is because I lack support methods to fit the skin and the recovery speed of the PUA substrate is not fast enough for us to find information about blood pressure response from the experimental results. In follow-up studies, I may need to re-select a substrate material that has a faster recovery speed and applicable for printing technology, so that I can finally effectuate blood pressure monitoring by improving design of the device and supporting methods.

BIBLIOGRAPHY

BIBLIOGRAPHY

- [1] B. D. Gates, “Flexible electronics,” *Science*, vol. 323, no. 5921, pp. 1566–1567, 2009.
- [2] A. Sandström, H. F. Dam, F. C. Krebs, and L. Edman, “Ambient fabrication of flexible and large-area organic light-emitting devices using slot-die coating,” *Nature communications*, vol. 3, p. 1002, 2012.
- [3] S. R. Forrest, “The path to ubiquitous and low-cost organic electronic appliances on plastic,” *Nature*, vol. 428, no. 6986, p. 911, 2004.
- [4] H. Sirringhaus, T. Kawase, R. Friend, T. Shimoda, M. Inbasekaran, W. Wu, and E. Woo, “High-resolution inkjet printing of all-polymer transistor circuits,” *Science*, vol. 290, no. 5499, pp. 2123–2126, 2000.
- [5] W.-Y. Chang, T.-H. Fang, H.-J. Lin, Y.-T. Shen, and Y.-C. Lin, “A large area flexible array sensors using screen printing technology,” *Journal of display technology*, vol. 5, no. 6, pp. 178–183, 2009.
- [6] M. Jung, J. Kim, J. Noh, N. Lim, C. Lim, G. Lee, J. Kim, H. Kang, K. Jung, A. D. Leonard, *et al.*, “All-printed and roll-to-roll-printable 13.56-mhz-operated 1-bit rf tag on plastic foils,” *IEEE Transactions on Electron Devices*, vol. 57, no. 3, pp. 571–580, 2010.
- [7] F. C. Krebs, “Fabrication and processing of polymer solar cells: a review of printing and coating techniques,” *Solar energy materials and solar cells*, vol. 93, no. 4, pp. 394–412, 2009.
- [8] R. H. Reuss, B. R. Chalamala, A. Moussessian, M. G. Kane, A. Kumar, D. C. Zhang, J. A. Rogers, M. Hatalis, D. Temple, G. Moddel, *et al.*, “Macroelectronics: Perspectives on technology and applications,” *Proceedings of the IEEE*, vol. 93, no. 7, pp. 1239–1256, 2005.
- [9] W. S. Wong and A. Salleo, *Flexible electronics: materials and applications*, vol. 11. Springer Science & Business Media, 2009.
- [10] N. Bowden, S. Brittain, A. G. Evans, J. W. Hutchinson, and G. M. Whitesides, “Spontaneous formation of ordered structures in thin films of metals supported on an elastomeric polymer,” *Nature*, vol. 393, no. 6681, p. 146, 1998.
- [11] T. W. Kelley, P. F. Baude, C. Gerlach, D. E. Ender, D. Muyres, M. A. Haase, D. E. Vogel, and S. D. Theiss, “Recent progress in organic electronics: Materials, devices, and processes,” *Chemistry of Materials*, vol. 16, no. 23, pp. 4413–4422, 2004.
- [12] B. Crone, A. Dodabalapur, Y.-Y. Lin, R. Filas, Z. Bao, A. LaDuca, R. Sarpeshkar, H. Katz, and W. Li, “Large-scale complementary integrated circuits based on organic transistors,” *Nature*, vol. 403, no. 6769, p. 521, 2000.

- [13] S. R. Forrest, “The path to ubiquitous and low-cost organic electronic appliances on plastic,” *Nature*, vol. 428, no. 6986, p. 911, 2004.
- [14] D.-Y. Khang, H. Jiang, Y. Huang, and J. A. Rogers, “A stretchable form of single-crystal silicon for high-performance electronics on rubber substrates,” *Science*, vol. 311, no. 5758, pp. 208–212, 2006.
- [15] Y. Zhang, S. Xu, H. Fu, J. Lee, J. Su, K.-C. Hwang, J. A. Rogers, and Y. Huang, “Buckling in serpentine microstructures and applications in elastomer-supported ultra-stretchable electronics with high areal coverage,” *Soft Matter*, vol. 9, no. 33, pp. 8062–8070, 2013.
- [16] Y. Zhang, S. Xu, H. Fu, J. Lee, J. Su, K.-C. Hwang, J. A. Rogers, and Y. Huang, “Buckling in serpentine microstructures and applications in elastomer-supported ultra-stretchable electronics with high areal coverage,” *Soft Matter*, vol. 9, no. 33, pp. 8062–8070, 2013.
- [17] J. Song, H. Jiang, W. Choi, D. Khang, Y. Huang, and J. Rogers, “An analytical study of two-dimensional buckling of thin films on compliant substrates,” *Journal of Applied Physics*, vol. 103, no. 1, p. 014303, 2008.
- [18] H. Jiang, D.-Y. Khang, J. Song, Y. Sun, Y. Huang, and J. A. Rogers, “Finite deformation mechanics in buckled thin films on compliant supports,” *Proceedings of the National Academy of Sciences*, vol. 104, no. 40, pp. 15607–15612, 2007.
- [19] H. Jiang, Y. Sun, J. A. Rogers, and Y. Huang, “Post-buckling analysis for the precisely controlled buckling of thin film encapsulated by elastomeric substrates,” *International Journal of Solids and Structures*, vol. 45, no. 7-8, pp. 2014–2023, 2008.
- [20] H. Jiang, Y. Sun, J. A. Rogers, and Y. Huang, “Mechanics of precisely controlled thin film buckling on elastomeric substrate,” *Applied physics letters*, vol. 90, no. 13, p. 133119, 2007.
- [21] H. C. Ko, M. P. Stoykovich, J. Song, V. Malyarchuk, W. M. Choi, C.-J. Yu, J. B. Geddes Iii, J. Xiao, S. Wang, Y. Huang, *et al.*, “A hemispherical electronic eye camera based on compressible silicon optoelectronics,” *Nature*, vol. 454, no. 7205, p. 748, 2008.
- [22] A. J. Baca, M. A. Meitl, H. C. Ko, S. Mack, H.-S. Kim, J. Dong, P. M. Ferreira, and J. A. Rogers, “Printable single-crystal silicon micro/nanoscale ribbons, platelets and bars generated from bulk wafers,” *Advanced Functional Materials*, vol. 17, no. 16, pp. 3051–3062, 2007.
- [23] A. Carlson, A. M. Bowen, Y. Huang, R. G. Nuzzo, and J. A. Rogers, “Transfer printing techniques for materials assembly and micro/nanodevice fabrication,” *Advanced Materials*, vol. 24, no. 39, pp. 5284–5318, 2012.
- [24] R. Saeidpourazar, R. Li, Y. Li, M. D. Sangid, C. Lu, Y. Huang, J. A. Rogers, and P. M. Ferreira, “Laser-driven micro transfer placement of prefabricated microstructures,” *Journal of Microelectromechanical Systems*, vol. 21, no. 5, pp. 1049–1058, 2012.

- [25] J. A. Rogers, “Nanometer-scale printing,” *Science*, vol. 337, no. 6101, pp. 1459–1460, 2012.
- [26] J.-H. Ahn, H.-S. Kim, E. Menard, K. J. Lee, Z. Zhu, D.-H. Kim, R. G. Nuzzo, J. A. Rogers, I. Amlani, V. Kushner, *et al.*, “Bendable integrated circuits on plastic substrates by use of printed ribbons of single-crystalline silicon,” *Applied Physics Letters*, vol. 90, no. 21, p. 213501, 2007.
- [27] H. Yang, D. Zhao, J.-H. Seo, S. Chuwongin, S. Kim, J. A. Rogers, Z. Ma, and W. Zhou, “Broadband membrane reflectors on glass,” *IEEE Photonics Technology Letters*, vol. 24, no. 6, pp. 476–478, 2012.
- [28] J. C. Shin, P. K. Mohseni, K. J. Yu, S. Tomasulo, K. H. Montgomery, M. L. Lee, J. A. Rogers, and X. Li, “Heterogeneous integration of ingaas nanowires on the rear surface of si solar cells for efficiency enhancement,” *ACS nano*, vol. 6, no. 12, pp. 11074–11079, 2012.
- [29] E. Bodenstein, S. Saager, M. Schober, C. Metzner, and U. Vogel, “P-208l: Late-news poster: Electron beam induced high-resolution modification of oled emission,” in *SID Symposium Digest of Technical Papers*, vol. 47, pp. 1802–1804, Wiley Online Library, 2016.
- [30] S. Wagner, S. P. Lacour, P.-H. Hsu, J. Sturm, and Z. Suo, “Stretchable and deformable macroelectronics,” in *Device Research Conference, 2003*, pp. 195–197, IEEE, 2003.
- [31] S. P. Lacour, J. Jones, S. Wagner, T. Li, and Z. Suo, “Stretchable interconnects for elastic electronic surfaces,” *Proceedings of the IEEE*, vol. 93, no. 8, pp. 1459–1467, 2005.
- [32] J. Jones, S. P. Lacour, S. Wagner, and Z. Suo, “Stretchable wavy metal interconnects,” *Journal of Vacuum Science & Technology A: Vacuum, Surfaces, and Films*, vol. 22, no. 4, pp. 1723–1725, 2004.
- [33] T. Li and Z. Suo, “Deformability of thin metal films on elastomer substrates,” *International Journal of Solids and Structures*, vol. 43, no. 7-8, pp. 2351–2363, 2006.
- [34] Z. Suo, J. Prevost, and J. Liang, “Kinetics of crack initiation and growth in organic-containing integrated structures,” *Journal of the Mechanics and Physics of Solids*, vol. 51, no. 11-12, pp. 2169–2190, 2003.
- [35] J. Wu, M. Li, W.-Q. Chen, D.-H. Kim, Y.-S. Kim, Y.-G. Huang, K.-C. Hwang, Z. Kang, and J. A. Rogers, “A strain-isolation design for stretchable electronics,” *Acta Mechanica Sinica*, vol. 26, no. 6, pp. 881–888, 2010.
- [36] H. Cheng, J. Wu, M. Li, D.-H. Kim, Y.-S. Kim, Y. Huang, Z. Kang, K. Hwang, and J. Rogers, “An analytical model of strain isolation for stretchable and flexible electronics,” *Applied Physics Letters*, vol. 98, no. 6, p. 061902, 2011.

- [37] H. Cheng, M. Li, J. Wu, A. Carlson, S. Kim, Y. Huang, Z. Kang, K.-C. Hwang, and J. Rogers, “A viscoelastic model for the rate effect in transfer printing,” *Journal of Applied Mechanics*, vol. 80, no. 4, p. 041019, 2013.
- [38] J. Xiao, A. Carlson, Z. Liu, Y. Huang, and J. Rogers, “Analytical and experimental studies of the mechanics of deformation in a solid with a wavy surface profile,” *Journal of applied Mechanics*, vol. 77, no. 1, p. 011003, 2010.
- [39] I. Jung, J. Xiao, V. Malyarchuk, C. Lu, M. Li, Z. Liu, J. Yoon, Y. Huang, and J. A. Rogers, “Dynamically tunable hemispherical electronic eye camera system with adjustable zoom capability,” *Proceedings of the National Academy of Sciences*, vol. 108, no. 5, pp. 1788–1793, 2011.
- [40] J. Song, Y. Huang, J. Xiao, S. Wang, K. Hwang, H. Ko, D.-H. Kim, M. Stoykovich, and J. Rogers, “Mechanics of noncoplanar mesh design for stretchable electronic circuits,” *Journal of Applied Physics*, vol. 105, no. 12, p. 123516, 2009.
- [41] G. Qin, J.-H. Seo, Y. Zhang, H. Zhou, W. Zhou, Y. Wang, J. Ma, and Z. Ma, “Rf characterization of gigahertz flexible silicon thin-film transistor on plastic substrates under bending conditions,” *IEEE Electron Device Letters*, vol. 34, no. 2, pp. 262–264, 2013.
- [42] G. Qin, H.-C. Yuan, Y. Qin, J.-H. Seo, Y. Wang, J. Ma, and Z. Ma, “Fabrication and characterization of flexible microwave single-crystal germanium nanomembrane diodes on a plastic substrate,” *IEEE Electron Device Letters*, vol. 34, no. 2, pp. 160–162, 2013.
- [43] H. Zhou, J.-H. Seo, D. M. Paskiewicz, Y. Zhu, G. K. Celler, P. M. Voyles, W. Zhou, M. G. Lagally, and Z. Ma, “Fast flexible electronics with strained silicon nanomembranes,” *Scientific reports*, vol. 3, p. 1291, 2013.
- [44] J.-H. Seo, J. Park, D. Zhao, H. Yang, W. Zhou, B.-K. Ju, and Z. Ma, “Large-area printed broadband membrane reflectors by laser interference lithography,” *IEEE Photonics Journal*, vol. 5, no. 1, pp. 2200106–2200106, 2013.
- [45] G. Gui, J. Zhong, and Z. Ma, “Electronic properties of rippled graphene,” in *Journal of Physics: Conference Series*, vol. 402, p. 012004, IOP Publishing, 2012.
- [46] T. A. Carstens, M. L. Corradini, J. P. Blanchard, and Z. Ma, “Thermoelectric powered wireless sensors for spent fuel monitoring,” *IEEE Transactions on Nuclear Science*, vol. 59, no. 4, pp. 1408–1413, 2012.
- [47] W. Zhou, Z. Ma, S. Chuwongin, Y.-C. Shuai, J.-H. Seo, D. Zhao, H. Yang, and W. Yang, “Semiconductor nanomembranes for integrated silicon photonics and flexible photonics,” *Optical and Quantum Electronics*, vol. 44, no. 12-13, pp. 605–611, 2012.
- [48] B. Lahey, A. Girouard, W. Burleson, and R. Vertegaal, “Paperphone: understanding the use of bend gestures in mobile devices with flexible electronic paper displays,” in *Proceedings of the SIGCHI Conference on Human Factors in Computing Systems*, pp. 1303–1312, ACM, 2011.

- [49] C. Ziegler, “Hp’s mckinney hints that a flexible display palm device could happen.,” 2016.
- [50] A. J. Bandothkar, W. Jia, C. Yardımcı, X. Wang, J. Ramirez, and J. Wang, “Tattoo-based noninvasive glucose monitoring: a proof-of-concept study,” *Analytical chemistry*, vol. 87, no. 1, pp. 394–398, 2014.
- [51] A. Miyamoto, S. Lee, N. F. Cooray, S. Lee, M. Mori, N. Matsuhisa, H. Jin, L. Yoda, T. Yokota, A. Itoh, *et al.*, “Inflammation-free, gas-permeable, lightweight, stretchable on-skin electronics with nanomeshes,” *Nature nanotechnology*, vol. 12, no. 9, p. 907, 2017.
- [52] D.-H. Kim, J.-H. Ahn, H.-S. Kim, K. J. Lee, T.-H. Kim, C.-J. Yu, R. G. Nuzzo, and J. A. Rogers, “Complementary logic gates and ring oscillators on plastic substrates by use of printed ribbons of single-crystalline silicon,” *IEEE Electron Device Letters*, vol. 29, no. 1, pp. 73–76, 2008.
- [53] Q. Cao, H.-s. Kim, N. Pimparkar, J. P. Kulkarni, C. Wang, M. Shim, K. Roy, M. A. Alam, and J. A. Rogers, “Medium-scale carbon nanotube thin-film integrated circuits on flexible plastic substrates,” *Nature*, vol. 454, no. 7203, p. 495, 2008.
- [54] M. Singh, H. M. Haverinen, P. Dhagat, and G. E. Jabbour, “Inkjet printing process and its applications,” *Advanced materials*, vol. 22, no. 6, pp. 673–685, 2010.
- [55] Z. Yin, Y. Huang, N. Bu, X. Wang, and Y. Xiong, “Inkjet printing for flexible electronics: Materials, processes and equipments,” *Chinese Science Bulletin*, vol. 55, no. 30, pp. 3383–3407, 2010.
- [56] H. Schiff, “Nanoimprint lithography: An old story in modern times? a review,” *Journal of Vacuum Science & Technology B: Microelectronics and Nanometer Structures Processing, Measurement, and Phenomena*, vol. 26, no. 2, pp. 458–480, 2008.
- [57] A. Carlson, A. M. Bowen, Y. Huang, R. G. Nuzzo, and J. A. Rogers, “Transfer printing techniques for materials assembly and micro/nanodevice fabrication,” *Advanced Materials*, vol. 24, no. 39, pp. 5284–5318, 2012.
- [58] A. Perl, D. N. Reinhoudt, and J. Huskens, “Microcontact printing: limitations and achievements,” *Advanced Materials*, vol. 21, no. 22, pp. 2257–2268, 2009.
- [59] R. R. Søndergaard, M. Hösel, and F. C. Krebs, “Roll-to-roll fabrication of large area functional organic materials,” *Journal of Polymer Science Part B: Polymer Physics*, vol. 51, no. 1, pp. 16–34, 2013.
- [60] S. Khan, L. Lorenzelli, and R. S. Dahiya, “Technologies for printing sensors and electronics over large flexible substrates: a review,” *IEEE Sensors Journal*, vol. 15, no. 6, pp. 3164–3185, 2015.
- [61] A. Sandström, H. F. Dam, F. C. Krebs, and L. Edman, “Ambient fabrication of flexible and large-area organic light-emitting devices using slot-die coating,” *Nature communications*, vol. 3, p. 1002, 2012.

- [62] M. Jung, J. Kim, J. Noh, N. Lim, C. Lim, G. Lee, J. Kim, H. Kang, K. Jung, A. D. Leonard, *et al.*, “All-printed and roll-to-roll-printable 13.56-mhz-operated 1-bit rf tag on plastic foils,” *IEEE Transactions on Electron Devices*, vol. 57, no. 3, pp. 571–580, 2010.
- [63] H. W. Kang, H. J. Sung, T.-M. Lee, D.-S. Kim, and C.-J. Kim, “Liquid transfer between two separating plates for micro-gravure-offset printing,” *Journal of Micromechanics and microengineering*, vol. 19, no. 1, p. 015025, 2008.
- [64] D. Deganello, J. Cherry, D. Gethin, and T. Claypole, “Patterning of micro-scale conductive networks using reel-to-reel flexographic printing,” *Thin Solid Films*, vol. 518, no. 21, pp. 6113–6116, 2010.
- [65] T. Kaufmann and B. J. Ravoo, “Stamps, inks and substrates: polymers in microcontact printing,” *Polymer Chemistry*, vol. 1, no. 4, pp. 371–387, 2010.
- [66] B. Radha, S. H. Lim, M. S. Saifullah, and G. U. Kulkarni, “Metal hierarchical patterning by direct nanoimprint lithography,” *Scientific reports*, vol. 3, p. 1078, 2013.
- [67] V. Subramanian, J. B. Chang, A. de la Fuente Vornbrock, D. C. Huang, L. Jagannathan, F. Liao, B. Mattis, S. Molesa, D. R. Redinger, D. Soltman, *et al.*, “Printed electronics for low-cost electronic systems: Technology status and application development,” in *Solid-State Device Research Conference, 2008. ESSDERC 2008. 38th European*, pp. 17–24, IEEE, 2008.
- [68] M. A. Leenen, V. Arning, H. Thiem, J. Steiger, and R. Anselmann, “Printable electronics: flexibility for the future,” *physica status solidi (a)*, vol. 206, no. 4, pp. 588–597, 2009.
- [69] D. Tobjörk and R. Österbacka, “Paper electronics,” *Advanced Materials*, vol. 23, no. 17, pp. 1935–1961, 2011.
- [70] P. F. Moonen, I. Yakimets, and J. Huskens, “Fabrication of transistors on flexible substrates: from mass-printing to high-resolution alternative lithography strategies,” *Advanced materials*, vol. 24, no. 41, pp. 5526–5541, 2012.
- [71] R. F. Pease and S. Y. Chou, “Lithography and other patterning techniques for future electronics,” *Proceedings of the IEEE*, vol. 96, no. 2, pp. 248–270, 2008.
- [72] A. Nathan, A. Ahnood, M. T. Cole, S. Lee, Y. Suzuki, P. Hiralal, F. Bonaccorso, T. Hasan, L. Garcia-Gancedo, A. Dyadyusha, *et al.*, “Flexible electronics: the next ubiquitous platform,” *Proceedings of the IEEE*, vol. 100, no. Special Centennial Issue, pp. 1486–1517, 2012.
- [73] A. Dodabalapur, “Organic and polymer transistors for electronics,” *Materials Today*, vol. 9, no. 4, pp. 24–30, 2006.
- [74] M.-C. Choi, Y. Kim, and C.-S. Ha, “Polymers for flexible displays: From material selection to device applications,” *Progress in Polymer Science*, vol. 33, no. 6, pp. 581–630, 2008.

- [75] Y. Sun and J. A. Rogers, “Inorganic semiconductors for flexible electronics,” *Advanced materials*, vol. 19, no. 15, pp. 1897–1916, 2007.
- [76] A. L. Dearden, P. J. Smith, D.-Y. Shin, N. Reis, B. Derby, and P. O’Brien, “A low curing temperature silver ink for use in ink-jet printing and subsequent production of conductive tracks,” *Macromolecular Rapid Communications*, vol. 26, no. 4, pp. 315–318, 2005.
- [77] B. K. Park, D. Kim, S. Jeong, J. Moon, and J. S. Kim, “Direct writing of copper conductive patterns by ink-jet printing,” *Thin Solid Films*, vol. 515, no. 19, pp. 7706–7711, 2007.
- [78] H.-H. Lee, K.-S. Chou, and K.-C. Huang, “Inkjet printing of nanosized silver colloids,” *Nanotechnology*, vol. 16, no. 10, p. 2436, 2005.
- [79] S. Magdassi, A. Bassa, Y. Vinetsky, and A. Kamyshny, “Silver nanoparticles as pigments for water-based ink-jet inks,” *Chemistry of Materials*, vol. 15, no. 11, pp. 2208–2217, 2003.
- [80] K. Kordás, T. Mustonen, G. Tóth, H. Jantunen, M. Lajunen, C. Soldano, S. Talapatra, S. Kar, R. Vajtai, and P. M. Ajayan, “Inkjet printing of electrically conductive patterns of carbon nanotubes,” *Small*, vol. 2, no. 8-9, pp. 1021–1025, 2006.
- [81] T. Wei, J. Ruan, Z. Fan, G. Luo, and F. Wei, “Preparation of a carbon nanotube film by ink-jet printing,” *Carbon*, vol. 45, no. 13, pp. 2712–2716, 2007.
- [82] F. Torrisi, T. Hasan, W. Wu, Z. Sun, A. Lombardo, T. S. Kulmala, G.-W. Hsieh, S. Jung, F. Bonaccorso, P. J. Paul, *et al.*, “Inkjet-printed graphene electronics,” *ACS nano*, vol. 6, no. 4, pp. 2992–3006, 2012.
- [83] R. S. Dahiya, G. Metta, M. Valle, and G. Sandini, “Tactile sensing from humans to humanoids,” *IEEE transactions on robotics*, vol. 26, no. 1, pp. 1–20, 2010.
- [84] R. S. Dahiya, D. Cattin, A. Adami, C. Collini, L. Barboni, M. Valle, L. Lorenzelli, R. Oboe, G. Metta, and F. Brunetti, “Towards tactile sensing system on chip for robotic applications,” *IEEE Sensors Journal*, vol. 11, no. 12, pp. 3216–3226, 2011.
- [85] R. S. Dahiya, P. Mittendorfer, M. Valle, G. Cheng, and V. J. Lumelsky, “Directions toward effective utilization of tactile skin: A review,” *IEEE Sensors Journal*, vol. 13, no. 11, pp. 4121–4138, 2013.
- [86] R. S. Dahiya, A. Adami, L. Pinna, C. Collini, M. Valle, and L. Lorenzelli, “Tactile sensing chips with posfet array and integrated interface electronics,” *IEEE Sensors Journal*, vol. 14, no. 10, pp. 3448–3457, 2014.
- [87] R. S. Dahiya and M. Valle, “Tactile sensing technologies,” in *Robotic tactile sensing*, pp. 79–136, Springer, 2013.

- [88] J. Perelaer, B.-J. de Gans, and U. S. Schubert, “Ink-jet printing and microwave sintering of conductive silver tracks,” *Advanced materials*, vol. 18, no. 16, pp. 2101–2104, 2006.
- [89] W. Shen, X. Zhang, Q. Huang, Q. Xu, and W. Song, “Preparation of solid silver nanoparticles for inkjet printed flexible electronics with high conductivity,” *Nanoscale*, vol. 6, no. 3, pp. 1622–1628, 2014.
- [90] T. Ohlund, A. K. Schuppert, M. Hummelgard, J. Backstrom, H.-E. Nilsson, and H. Olin, “Inkjet fabrication of copper patterns for flexible electronics: using paper with active precoatings,” *ACS applied materials & interfaces*, vol. 7, no. 33, pp. 18273–18282, 2015.
- [91] Z. Zhang, X. Zhang, Z. Xin, M. Deng, Y. Wen, and Y. Song, “Synthesis of monodisperse silver nanoparticles for ink-jet printed flexible electronics,” *Nanotechnology*, vol. 22, no. 42, p. 425601, 2011.
- [92] M. Terrones, A. Jorio, M. Endo, A. Rao, Y. Kim, T. Hayashi, H. Terrones, J.-C. Charlier, G. Dresselhaus, and M. Dresselhaus, “New direction in nanotube science,” *Materials Today*, vol. 7, no. 10, pp. 30–45, 2004.
- [93] Z. Fan, T. Wei, G. Luo, and F. Wei, “Fabrication and characterization of multi-walled carbon nanotubes-based ink,” *Journal of materials science*, vol. 40, no. 18, pp. 5075–5077, 2005.
- [94] T. Wei, J. Ruan, Z. Fan, G. Luo, and F. Wei, “Preparation of a carbon nanotube film by ink-jet printing,” *Carbon*, vol. 45, no. 13, pp. 2712–2716, 2007.
- [95] K. S. Novoselov, V. Fal, L. Colombo, P. Gellert, M. Schwab, K. Kim, *et al.*, “A roadmap for graphene,” *Nature*, vol. 490, no. 7419, p. 192, 2012.
- [96] Y. Seekaew, S. Lokavee, D. Phokharatkul, A. Wisitsoraat, T. Kerdcharoen, and C. Wongchoosuk, “Low-cost and flexible printed graphene–pedot: Pss gas sensor for ammonia detection,” *Organic Electronics*, vol. 15, no. 11, pp. 2971–2981, 2014.
- [97] W. A. MacDonald, M. Looney, D. MacKerron, R. Eveson, R. Adam, K. Hashimoto, and K. Rakos, “Latest advances in substrates for flexible electronics,” *Journal of the Society for Information Display*, vol. 15, no. 12, pp. 1075–1083, 2007.
- [98] V. Zardetto, T. M. Brown, A. Reale, and A. Di Carlo, “Substrates for flexible electronics: A practical investigation on the electrical, film flexibility, optical, temperature, and solvent resistance properties,” *Journal of Polymer Science Part B: Polymer Physics*, vol. 49, no. 9, pp. 638–648, 2011.
- [99] S. Nambiar and J. T. Yeow, “Conductive polymer-based sensors for biomedical applications,” *Biosensors and Bioelectronics*, vol. 26, no. 5, pp. 1825–1832, 2011.

- [100] A. C. Arias, J. Daniel, S. Sambandan, T. N. Ng, B. Russo, B. Krusor, and R. A. Street, “All printed thin film transistors for flexible electronics,” in *Organic Field-Effect Transistors VII and Organic Semiconductors in Sensors and Bioelectronics*, vol. 7054, p. 70540L, International Society for Optics and Photonics, 2008.
- [101] S. Nishi, K. Asano, D. Ishibashi, A. Kitami, and K. Furuno, “Printed electronics on flexible substrate using inkjet technology,” *Transactions of The Japan Institute of Electronics Packaging*, vol. 2, no. 1, pp. 75–78, 2009.
- [102] S. H. Ko, H. Pan, C. P. Grigoropoulos, C. K. Luscombe, J. M. Fréchet, and D. Poulikakos, “All-inkjet-printed flexible electronics fabrication on a polymer substrate by low-temperature high-resolution selective laser sintering of metal nanoparticles,” *Nanotechnology*, vol. 18, no. 34, p. 345202, 2007.
- [103] J. A. Rogers, T. Someya, and Y. Huang, “Materials and mechanics for stretchable electronics,” *science*, vol. 327, no. 5973, pp. 1603–1607, 2010.
- [104] S. Choi, J. Park, W. Hyun, J. Kim, J. Kim, Y. B. Lee, C. Song, H. J. Hwang, J. H. Kim, T. Hyeon, *et al.*, “Stretchable heater using ligand-exchanged silver nanowire nanocomposite for wearable articular thermotherapy,” *ACS nano*, vol. 9, no. 6, pp. 6626–6633, 2015.
- [105] S. Bae, H. Kim, Y. Lee, X. Xu, J.-S. Park, Y. Zheng, J. Balakrishnan, T. Lei, H. R. Kim, Y. I. Song, *et al.*, “Roll-to-roll production of 30-inch graphene films for transparent electrodes,” *Nature nanotechnology*, vol. 5, no. 8, p. 574, 2010.
- [106] Z. Niu, H. Dong, B. Zhu, J. Li, H. H. Hng, W. Zhou, X. Chen, and S. Xie, “Highly stretchable, integrated supercapacitors based on single-walled carbon nanotube films with continuous reticulate architecture,” *Advanced Materials*, vol. 25, no. 7, pp. 1058–1064, 2013.
- [107] D. J. Lipomi, J. A. Lee, M. Vosgueritchian, B. C.-K. Tee, J. A. Bolander, and Z. Bao, “Electronic properties of transparent conductive films of PEDOT:PSS on stretchable substrates,” *Chemistry of Materials*, vol. 24, no. 2, pp. 373–382, 2012.
- [108] Y. Kim, J. Zhu, B. Yeom, M. Di Prima, X. Su, J.-G. Kim, S. J. Yoo, C. Uher, and N. A. Kotov, “Stretchable nanoparticle conductors with self-organized conductive pathways,” *Nature*, vol. 500, no. 7460, p. 59, 2013.
- [109] S. Yao and Y. Zhu, “Nanomaterial-enabled stretchable conductors: strategies, materials and devices,” *Advanced Materials*, vol. 27, no. 9, pp. 1480–1511, 2015.
- [110] J. Liang, L. Li, K. Tong, Z. Ren, W. Hu, X. Niu, Y. Chen, and Q. Pei, “Silver nanowire percolation network soldered with graphene oxide at room temperature and its application for fully stretchable polymer light-emitting diodes,” *ACS nano*, vol. 8, no. 2, pp. 1590–1600, 2014.

- [111] S. Kang, T. Kim, S. Cho, Y. Lee, A. Choe, B. Walker, S.-J. Ko, J. Y. Kim, and H. Ko, “Capillary printing of highly aligned silver nanowire transparent electrodes for high-performance optoelectronic devices,” *Nano letters*, vol. 15, no. 12, pp. 7933–7942, 2015.
- [112] S. Yao and Y. Zhu, “Wearable multifunctional sensors using printed stretchable conductors made of silver nanowires,” *Nanoscale*, vol. 6, no. 4, pp. 2345–2352, 2014.
- [113] M. Singh, H. M. Haverinen, P. Dhagat, and G. E. Jabbour, “Inkjet printing process and its applications,” *Advanced materials*, vol. 22, no. 6, pp. 673–685, 2010.
- [114] B.-R. Yang, W. Cao, G.-S. Liu, H.-J. Chen, Y.-Y. Noh, T. Minari, H.-C. Hsiao, C.-Y. Lee, H.-P. D. Shieh, and C. Liu, “Microchannel wetting for controllable patterning and alignment of silver nanowire with high resolution,” *ACS applied materials & interfaces*, vol. 7, no. 38, pp. 21433–21441, 2015.
- [115] D. J. Finn, M. Lotya, and J. N. Coleman, “Inkjet printing of silver nanowire networks,” *ACS applied materials & interfaces*, vol. 7, no. 17, pp. 9254–9261, 2015.
- [116] S.-P. Chen, J. R. D. Retamal, D.-H. Lien, J.-H. He, and Y.-C. Liao, “Inkjet-printed transparent nanowire thin film features for uv photodetectors,” *RSC Advances*, vol. 5, no. 87, pp. 70707–70712, 2015.
- [117] H. Lee, B. Seong, J. Kim, Y. Jang, and D. Byun, “Direct alignment and patterning of silver nanowires by electrohydrodynamic jet printing,” *Small*, vol. 10, no. 19, pp. 3918–3922, 2014.
- [118] B. Lahey, A. Girouard, W. Burleson, and R. Vertegaal, “Paperphone: understanding the use of bend gestures in mobile devices with flexible electronic paper displays,” in *Proceedings of the SIGCHI Conference on Human Factors in Computing Systems*, pp. 1303–1312, ACM, 2011.
- [119] D. Vij, “Series on optics and optoelectronics, handbook of electroluminescent materials,” 2004.
- [120] S. Zhang, *Fully Printed Flexible and Stretchable Electronics*. PhD thesis, Michigan State University, 2018.
- [121] S. Li, B. N. Peele, C. M. Larson, H. Zhao, and R. F. Shepherd, “A stretchable multicolor display and touch interface using photopatterning and transfer printing,” *Advanced Materials*, vol. 28, no. 44, pp. 9770–9775, 2016.
- [122] D.-H. Kim, N. Lu, R. Ma, Y.-S. Kim, R.-H. Kim, S. Wang, J. Wu, S. M. Won, H. Tao, A. Islam, *et al.*, “Epidermal electronics,” *science*, vol. 333, no. 6044, pp. 838–843, 2011.
- [123] S. C. Mannsfeld, B. C. Tee, R. M. Stoltenberg, C. V. H. Chen, S. Barman, B. V. Muir, A. N. Sokolov, C. Reese, and Z. Bao, “Highly sensitive flexible pressure sensors with microstructured rubber dielectric layers,” *Nature materials*, vol. 9, no. 10, p. 859, 2010.

- [124] G. Schwartz, B. C.-K. Tee, J. Mei, A. L. Appleton, D. H. Kim, H. Wang, and Z. Bao, “Flexible polymer transistors with high pressure sensitivity for application in electronic skin and health monitoring,” *Nature communications*, vol. 4, p. 1859, 2013.
- [125] K. Takei, T. Takahashi, J. C. Ho, H. Ko, A. G. Gillies, P. W. Leu, R. S. Fearing, and A. Javey, “Nanowire active-matrix circuitry for low-voltage macroscale artificial skin,” *Nature materials*, vol. 9, no. 10, p. 821, 2010.
- [126] M. Kaltenbrunner, T. Sekitani, J. Reeder, T. Yokota, K. Kuribara, T. Tokuhara, M. Drack, R. Schwödianer, I. Graz, S. Bauer-Gogonea, *et al.*, “An ultra-lightweight design for imperceptible plastic electronics,” *Nature*, vol. 499, no. 7459, p. 458, 2013.
- [127] C. Wang, D. Hwang, Z. Yu, K. Takei, J. Park, T. Chen, B. Ma, and A. Javey, “User-interactive electronic skin for instantaneous pressure visualization,” *Nature materials*, vol. 12, no. 10, p. 899, 2013.
- [128] J.-W. Jeong, W.-H. Yeo, A. Akhtar, J. J. Norton, Y.-J. Kwack, S. Li, S.-Y. Jung, Y. Su, W. Lee, J. Xia, *et al.*, “Materials and optimized designs for human-machine interfaces via epidermal electronics,” *Advanced Materials*, vol. 25, no. 47, pp. 6839–6846, 2013.
- [129] D. J. Lipomi, M. Vosgueritchian, B. C. Tee, S. L. Hellstrom, J. A. Lee, C. H. Fox, and Z. Bao, “Skin-like pressure and strain sensors based on transparent elastic films of carbon nanotubes,” *Nature nanotechnology*, vol. 6, no. 12, p. 788, 2011.
- [130] F.-R. Fan, L. Lin, G. Zhu, W. Wu, R. Zhang, and Z. L. Wang, “Transparent triboelectric nanogenerators and self-powered pressure sensors based on micropatterned plastic films,” *Nano letters*, vol. 12, no. 6, pp. 3109–3114, 2012.
- [131] T. Someya, T. Sekitani, S. Iba, Y. Kato, H. Kawaguchi, and T. Sakurai, “A large-area, flexible pressure sensor matrix with organic field-effect transistors for artificial skin applications,” *Proceedings of the National Academy of Sciences of the United States of America*, vol. 101, no. 27, pp. 9966–9970, 2004.
- [132] M. Cheng, X. Huang, C. Ma, and Y. Yang, “A flexible capacitive tactile sensing array with floating electrodes,” *Journal of Micromechanics and Microengineering*, vol. 19, no. 11, p. 115001, 2009.
- [133] Z. L. Wang and W. Wu, “Nanotechnology-enabled energy harvesting for self-powered micro-/nanosystems,” *Angewandte Chemie International Edition*, vol. 51, no. 47, pp. 11700–11721, 2012.
- [134] Y. Hu, J. Yang, Q. Jing, S. Niu, W. Wu, and Z. L. Wang, “Triboelectric nanogenerator built on suspended 3d spiral structure as vibration and positioning sensor and wave energy harvester,” *ACS nano*, vol. 7, no. 11, pp. 10424–10432, 2013.
- [135] D. J. Cohen, D. Mitra, K. Peterson, and M. M. Maharbiz, “A highly elastic, capacitive strain gauge based on percolating nanotube networks,” *Nano letters*, vol. 12, no. 4, pp. 1821–1825, 2012.

- [136] R. Matsuzaki, T. Keating, A. Todoroki, and N. Hiraoka, “Rubber-based strain sensor fabricated using photolithography for intelligent tires,” *Sensors and Actuators A: Physical*, vol. 148, no. 1, pp. 1–9, 2008.
- [137] Q. Gao, H. Meguro, S. Okamoto, and M. Kimura, “Flexible tactile sensor using the reversible deformation of poly (3-hexylthiophene) nanofiber assemblies,” *Langmuir*, vol. 28, no. 51, pp. 17593–17596, 2012.
- [138] J. Zhou, Y. Gu, P. Fei, W. Mai, Y. Gao, R. Yang, G. Bao, and Z. L. Wang, “Flexible piezotronic strain sensor,” *Nano letters*, vol. 8, no. 9, pp. 3035–3040, 2008.
- [139] D. Mandal, S. Yoon, and K. J. Kim, “Origin of piezoelectricity in an electrospun poly (vinylidene fluoride-trifluoroethylene) nanofiber web-based nanogenerator and nano-pressure sensor,” *Macromolecular rapid communications*, vol. 32, no. 11, pp. 831–837, 2011.
- [140] Y. Yang, H. Zhang, Z.-H. Lin, Y. S. Zhou, Q. Jing, Y. Su, J. Yang, J. Chen, C. Hu, and Z. L. Wang, “Human skin based triboelectric nanogenerators for harvesting biomechanical energy and as self-powered active tactile sensor system,” *ACS nano*, vol. 7, no. 10, pp. 9213–9222, 2013.
- [141] T. Yamada, Y. Hayamizu, Y. Yamamoto, Y. Yomogida, A. Izadi-Najafabadi, D. N. Futaba, and K. Hata, “A stretchable carbon nanotube strain sensor for human-motion detection,” *Nature nanotechnology*, vol. 6, no. 5, p. 296, 2011.
- [142] C. Pang, G.-Y. Lee, T.-i. Kim, S. M. Kim, H. N. Kim, S.-H. Ahn, and K.-Y. Suh, “A flexible and highly sensitive strain-gauge sensor using reversible interlocking of nanofibres,” *Nature materials*, vol. 11, no. 9, p. 795, 2012.
- [143] X. Xiao, L. Yuan, J. Zhong, T. Ding, Y. Liu, Z. Cai, Y. Rong, H. Han, J. Zhou, and Z. L. Wang, “High-strain sensors based on zno nanowire/polystyrene hybridized flexible films,” *Advanced materials*, vol. 23, no. 45, pp. 5440–5444, 2011.
- [144] L. Lin, Y. Xie, S. Wang, W. Wu, S. Niu, X. Wen, and Z. L. Wang, “Triboelectric active sensor array for self-powered static and dynamic pressure detection and tactile imaging,” *ACS nano*, vol. 7, no. 9, pp. 8266–8274, 2013.
- [145] M. Park, J. Im, J. Park, and U. Jeong, “Micropatterned stretchable circuit and strain sensor fabricated by lithography on an electrospun nanofiber mat,” *ACS applied materials & interfaces*, vol. 5, no. 17, pp. 8766–8771, 2013.
- [146] V. Maheshwari and R. F. Saraf, “High-resolution thin-film device to sense texture by touch,” *Science*, vol. 312, no. 5779, pp. 1501–1504, 2006.
- [147] M. Segev-Bar, A. Landman, M. Nir-Shapira, G. Shuster, and H. Haick, “Tunable touch sensor and combined sensing platform: Toward nanoparticle-based electronic skin,” *ACS applied materials & interfaces*, vol. 5, no. 12, pp. 5531–5541, 2013.

- [148] N. M. Sangeetha, N. Decorde, B. Viallet, G. Viau, and L. Ressier, “Nanoparticle-based strain gauges fabricated by convective self assembly: Strain sensitivity and hysteresis with respect to nanoparticle sizes,” *The Journal of Physical Chemistry C*, vol. 117, no. 4, pp. 1935–1940, 2013.
- [149] S. Gong, W. Schwalb, Y. Wang, Y. Chen, Y. Tang, J. Si, B. Shirinzadeh, and W. Cheng, “A wearable and highly sensitive pressure sensor with ultrathin gold nanowires,” *Nature communications*, vol. 5, p. 3132, 2014.
- [150] M. Su, F. Li, S. Chen, Z. Huang, M. Qin, W. Li, X. Zhang, and Y. Song, “Nanoparticle based curve arrays for multirecognition flexible electronics,” *Advanced Materials*, vol. 28, no. 7, pp. 1369–1374, 2016.
- [151] H. Shi, T. Pinto, Y. Zhang, C. Wang, and X. Tan, “Soft capacitive sensors for measurement of both positive and negative pressures,” in *Nano-, Bio-, Info-Tech Sensors, and 3D Systems II*, vol. 10597, p. 105971E, International Society for Optics and Photonics, 2018.